

Higgs Boson Decays to Dark Photons through the Vectorized Lepton Portal

Qianshu Lu^(a,b), David E. Morrissey^(a), and Alexander M. Wijangco^(a)

(a) TRIUMF, 4004 Wesbrook Mall, Vancouver, BC, Canada V6T 2A3

(b) Division of Engineering Science, University of Toronto, Toronto, ON, Canada M5S 2E4

email: qianshu.lu@mail.utoronto.ca, dmorri@triumf.ca, awijangco@triumf.ca

June 22, 2017

Abstract

Vector-like fermions charged under both the Standard Model and a new dark gauge group arise in many theories of new physics. If these fermions include an electroweak doublet and singlet with equal dark charges, they can potentially connect to the Higgs field through a Yukawa coupling in analogy to the standard neutrino portal. With such a coupling, fermion loops generate exotic decays of the Higgs boson to one or more dark vector bosons. In this work we study a minimal realization of this scenario with an Abelian dark group. We investigate the potential new Higgs decays modes, we compute their rates, and we study the prospects for observing them at the Large Hadron Collider and beyond given the other experimental constraints on the theory. We also discuss extensions of the theory to non-Abelian dark groups.

1 Introduction

Dark sectors have been studied extensively in recent years [1, 2, 3, 4, 5]. Such sectors consist of new states that interact only very weakly with the Standard Model (SM). This allows the new physics in the dark sector to be relatively light, with characteristic mass well below the electroweak scale, while still being consistent with current experimental tests. Dark sectors may also be related to (or comprise) the dark matter in the universe [6, 7, 8, 9].

While the range of possibilities for dark sectors is enormous, particular attention has been given to those that connect to the SM through a set of portal operators:

$$\text{Vector Portal :} \quad \frac{\epsilon}{2} B_{\mu\nu} X^{\mu\nu} \quad (1)$$

$$\text{Higgs Portal :} \quad (A\phi + \kappa\phi^2)|H|^2 \quad (2)$$

$$\text{Neutrino Portal :} \quad y_N \bar{L} \tilde{H} N \quad (3)$$

First, in the vector portal, a new Abelian vector boson X couples to the SM through kinetic mixing with hypercharge [10, 11]. Second, in the Higgs portal [12, 13], a new scalar connects with the SM Higgs field. And third, in the neutrino portal a new gauge singlet fermion N connects to the SM lepton and Higgs doublets. These portals represent the three ways in which a new field with no SM charges can couple to the SM at the renormalizable level. As such, these interactions are non-decoupling, and the most sensitive searches for light new physics connecting to us through these interactions are typically lower-energy experiments with very high intensity or precision [4].

The portal interactions of Eqs. (1,2,3) can be generated by integrating out massive *mediator* states that couple directly to both the visible and dark sectors. Such mediators can give rise to new and unusual signals at high-energy colliders such as the Large Hadron Collider (LHC), either through their direct production or by providing a new avenue to populate the light states in the dark sector [14, 15, 16]. Discovering mediator particles or measuring their decoupling effects would also provide new insight into the structure and dynamics of the light states in the dark sector.

In this paper we investigate a very simple theory of mediators to a dark sector consisting of a $U(1)_x$ vector boson X , first presented in Ref. [17]. The mediators are an electroweak singlet N and doublet P of Dirac fermions with hypercharges $Y = 0, -1/2$ and equal dark charge q_x . These quantum numbers allow for vector-like fermion masses and a coupling to the SM Higgs boson of the form

$$-\mathcal{L} \supset \lambda \bar{P} \tilde{H} N + (h.c.) , \quad (4)$$

where $\tilde{H} = i\sigma_2 H^*$. After electroweak symmetry breaking, the singlet and doublet mix to form a pair of neutral Dirac fermions ψ_1 and ψ_2 , and a charged fermion P^- . We assume as well that the dark vector boson develops a mass m_x , either through a dark sector Higgs or Stueckelberg mechanism [18, 19]. The interaction of Eq. (4) is analogous to the neutrino portal, but it involves the new $U(1)_x$ charged mediators instead of the SM leptons; we call it

the *vectorized lepton portal*. In addition to this portal interaction, loops of the new fermions also contribute to a vector portal coupling between the $U(1)_x$ vector boson and hypercharge.

This general structure appears in a broad range of proposed extensions of the SM. The new fermions in the theory have the same SM quantum numbers as some of the models of vector-like leptons (without dark charges) considered in Refs. [20, 21]. In theories with supersymmetry, superpotential couplings of the form of Eq. (4) are the origin of general renormalizable Higgs portal interactions via scalar F -terms, and they have been invoked to connect the Higgs to gauge mediator supermultiplets [22, 23] and to increase the mass of the SM-like Higgs boson [24, 25, 26]. Closely related structures with non-Abelian dark gauge groups also emerge in some theories of neutral naturalness such as folded supersymmetry [27] and quirky little Higgs [28], and in relaxion constructions [29, 30, 31, 32]. Realizations of the vectorized lepton portal with an Abelian dark group were studied in Refs. [17, 33, 34, 35], and with a non-Abelian group in Ref. [36, 37].

The vectorized lepton portal can induce a wide range of new experimental signals, both from the light dark vector and the heavier mediator fermions. The new signals of primary interest in this work are exotic decays of the SM Higgs boson. Loops of the vector-like fermions give rise to $h \rightarrow XX$ and $h \rightarrow XZ$ decay channels. We show that the resulting branching fractions can be much larger than from kinetic mixing alone. Furthermore, we also demonstrate that these decays are potentially observable at the LHC (and beyond) while being consistent with current bounds from precision electroweak tests and direct collider searches. Relative to the closely related previous works of Refs. [17, 33], we compute the Higgs decay widths and the direct constraints due to the new fermions in more detail, and we show that current direct limits allow for observable Higgs signals at the LHC.

Following this introduction, we present a simple vectorized lepton portal model in more detail in Sec. 2. Next, we calculate the Higgs boson decay widths to dark vectors through mediator fermion loops and discuss their observability at the LHC and beyond in Sec. 3. Constraints on the mediators from precision electroweak measurements, direct searches at the LHC, and stability of the Higgs potential are discussed in Sec. 4. In Sec. 5 we study the implications of the theory for dark matter and cosmology, and we discuss some potential extensions of the minimal theory motivated by them. Further extensions of the minimal theory to non-Abelian dark gauge groups are discussed in Sec. 6. Finally, we reserve Sec. 7 for our conclusions.

2 Fields, Masses, and Interactions

We consider a theory with two new vector-like fermion multiplets with charge assignments under $SU(3)_c \times SU(2)_L \times U(1)_Y \times U(1)_x$ of $N = (1, 1, 0; q_x)$ and $P = (1, 2, -1/2; q_x)$. This allows the Yukawa coupling and masses:

$$-\mathcal{L} \supset \left(\lambda \bar{P} \tilde{H} N + h.c. \right) + m_P \bar{P} P + m_N \bar{N} N , \quad (5)$$

where $\tilde{H} = i\sigma_2 H^*$. Note that m_P , m_N , and λ can all be taken to be real and positive through field redefinitions. We also normalize the dark gauge coupling g_x such that either $q_x = 1$ or $q_x = -1$. The set of fermion charges in our theory is minimal in that there is only one new (Dirac) field with SM gauge charges. Let us also mention that the Yukawa interaction of Eq. (5) can be generalized to a chiral form with two independent Yukawa couplings that allows for CP violation [38, 39, 40, 41]; we focus on the parity-preserving form of Eq. (5) for simplicity.

2.1 Minimal Masses and Interactions

Expanding the Higgs about its vacuum expectation value (VEV) in unitary gauge, $H \rightarrow (v + h/\sqrt{2})$, with $v = 174$ GeV, and writing the $SU(2)_L$ components of the doublet explicitly as $P = (P^0, P^-)^T$, the fermion terms become

$$-\mathcal{L} \supset -m_P \bar{P}^- P^- + (\bar{N}, \bar{P}^0) \begin{pmatrix} m_N & \lambda v \\ \lambda v & m_P \end{pmatrix} \begin{pmatrix} N \\ P^0 \end{pmatrix} + \frac{\lambda}{\sqrt{2}} h (\bar{N} P^0 + \bar{P}^0 N) . \quad (6)$$

The physical states are therefore a charged fermion P^- with mass m_P together with two SM-neutral Dirac fermions $\psi_{1,2}$ with masses

$$m_{1,2} = \frac{1}{2} \left[(m_N + m_P) \mp \sqrt{(m_N - m_P)^2 + 4\lambda^2 v^2} \right] . \quad (7)$$

We only consider solutions with positive $m_1 > 0$ in this work, corresponding to the condition $\sqrt{m_N m_P} > \lambda v$, since the $m_1 < 0$ solution has $|m_1| \leq \lambda v$ and is strongly constrained by direct searches. The neutral gauge eigenstates are related to the mass eigenstates by

$$\begin{pmatrix} N \\ P^0 \end{pmatrix} = \begin{pmatrix} c_\alpha & s_\alpha \\ -s_\alpha & c_\alpha \end{pmatrix} \begin{pmatrix} \psi_1 \\ \psi_2 \end{pmatrix} . \quad (8)$$

with the mixing angle given by

$$\tan(2\alpha) = \frac{2\lambda v}{m_P - m_N} . \quad (9)$$

We choose the solution for α such that $m_1 < m_2$.

Rewriting the Yukawa interaction in terms of the mass eigenstates, we find

$$-\mathcal{L} \supset \frac{\lambda}{\sqrt{2}} h \left[2s_\alpha c_\alpha (-\bar{\psi}_1 \psi_1 + \bar{\psi}_2 \psi_2) + (c_\alpha^2 - s_\alpha^2) (\bar{\psi}_1 \psi_2 + \bar{\psi}_2 \psi_1) \right] . \quad (10)$$

Note that the charged P^- state does not couple to the Higgs boson. The relevant vector boson couplings are

$$\begin{aligned} -\mathcal{L} \supset & \bar{g} \left(-\frac{1}{2} + s_W^2 \right) Z_\mu \bar{P}^- \gamma^\mu P^- - e A_\mu \bar{P}^- \gamma^\mu P^- \\ & + \frac{g}{\sqrt{2}} \left[W_\mu^+ \bar{P}^- \gamma^\mu (-s_\alpha \psi_1 + c_\alpha \psi_2) + (h.c.) \right] \\ & + \frac{1}{2} \bar{g} Z_\mu \left[s_\alpha^2 \bar{\psi}_1 \gamma^\mu \psi_1 + c_\alpha^2 \bar{\psi}_2 \gamma^\mu \psi_2 - s_\alpha c_\alpha (\bar{\psi}_1 \gamma^\mu \psi_2 + \bar{\psi}_2 \gamma^\mu \psi_1) \right] \\ & + g_x X_\mu \left[\bar{\psi}_1 \gamma_\mu \psi_1 + \bar{\psi}_2 \gamma_\mu \psi_2 + \bar{P}^- \gamma_\mu P^- \right] , \end{aligned} \quad (11)$$

where $\bar{g} = g/c_W = \sqrt{g^2 + g'^2}$.

Beyond the Yukawa and gauge couplings above, the dark sector also couples to the SM through gauge kinetic mixing [10, 11],

$$-\mathcal{L} \supset \frac{\epsilon}{2c_W} B_{\mu\nu} X^{\mu\nu} . \quad (12)$$

This interaction can be treated as in Refs. [2, 3, 42], with the main effect for $m_x \ll m_Z$ being kinetic mixing with the photon with strength ϵ . It allows the dark vector to decay to lighter SM final states.

We take ϵ to be an independent parameter, but it should be noted that it is generated by P loops. The log-enhanced running contribution to ϵ from these loops between scale μ and m_P is [43, 44]

$$\begin{aligned} \Delta\epsilon &\simeq -\frac{q_x}{3\pi} \sqrt{\alpha_x \alpha} \ln\left(\frac{\mu}{m_P}\right) \\ &\simeq -q_x (3 \times 10^{-3}) \left(\frac{\alpha_x}{10\alpha}\right)^{1/2} \ln\left(\frac{\mu}{m_P}\right) , \end{aligned} \quad (13)$$

where $\alpha_x = g_x^2/4\pi$. Values much smaller than this are expected to require some degree of tuning, or additional structure in the theory such as an approximately conserved charge conjugation symmetry in the dark sector [34].

2.2 Additional Interactions

Several other interactions can be added to the minimal set discussed above if the dark sector contains a scalar ϕ with dark charge Q_x , such as a dark Higgs boson responsible for generating the dark vector mass [17, 33]. For any Q_x , the scalar can connect to the SM Higgs field through the Higgs portal,

$$-\mathcal{L} \supset \kappa |\phi|^2 |H|^2 . \quad (14)$$

This will induce Higgs mixing if ϕ develops a VEV. Such an interaction is generated at two-loop order through the gauge and Yukawa couplings of the theory with size

$$\begin{aligned} \Delta\kappa &\sim \frac{Q_x^2}{(4\pi)^2} \lambda^2 \alpha_x^2 \\ &= (4 \times 10^{-5}) \left(\frac{\alpha_x}{10\alpha}\right)^2 \lambda^2 Q_x^2 . \end{aligned} \quad (15)$$

As for ϵ , we take this as a lower limit on the natural size of κ . It is parametrically smaller than the sizes of the effects we consider.

Other gauge invariant operators are possible for special values of the charge Q_x of ϕ [17, 33]. For $Q_x = \pm q_x$, a direct lepton mixing is allowed,

$$-\mathcal{L} \supset y_L \phi \bar{P}_R L_L + (h.c.) , \quad (16)$$

where L_L is the SM lepton doublet. This operator can contribute to lepton masses and flavor violation, but current bounds can typically be satisfied for couplings below $|y_L| \lesssim 10^{-3}$ [17]. With $Q_x = -2q_x$ we can write

$$-\mathcal{L} \supset y_N \phi \bar{N}^c N + (h.c.) , \quad (17)$$

which induces a Majorana mass for N (and a one-loop contribution to κ) for non-zero $\langle \phi \rangle$.

3 Higgs Boson Decays to Dark Vectors

Decays of the Higgs boson to one or more dark vectors are generated by the portal coupling of Eq. (4). These arise at one-loop order from UV-finite triangle diagrams, in direct analogy to the contributions to the SM Higgs decay modes $h \rightarrow \gamma\gamma$ and $h \rightarrow gg$ from loops of the top quark. In our minimal vectorized lepton portal scenario, the new decay channels are $h \rightarrow XX$ and $h \rightarrow XZ$. We investigate these decays in this section.

Before proceeding, let us also mention that the mediator fermions typically do not modify the Higgs branching fractions to SM final states in a significant way. There is no direct one-loop contribution to $h \rightarrow gg$ since the mediators are uncolored, and the absence of a tree-level coupling of the charged P^- mode to the Higgs implies the same for $h \rightarrow \gamma\gamma$ and $h \rightarrow \gamma X$. The primary exception to this occurs when the new fermions are light enough that $h \rightarrow \psi_1 \bar{\psi}_1$ is allowed. For λ of order unity, this channel can easily dominate the Higgs width. Since our focus is on decays of the Higgs to dark vectors, which require larger λ to be relevant, we concentrate on fermion masses greater than $m_1 > m_h/2$.

3.1 Higgs Branching Fractions

The vectorized lepton portal can induce both $h \rightarrow XX$ and $h \rightarrow XZ$ decays at a similar level. We collect in Appendix A the loop functions relevant for the decay. The asymptotic form of the $h \rightarrow XX$ decay in the limit $m_{1,2} \gg m_h$ and $m_x \rightarrow 0$ can be obtained as a low-energy Higgs theorem [45]. The result is

$$\mathcal{L}_{eff} \supset -\frac{1}{4} \frac{\alpha_x}{4\pi} \left(\sum_{i=1}^2 \Delta b_i \frac{2}{m_i} \frac{\partial m_i}{\partial v} \right) \left(\frac{h}{\sqrt{2}} \right) X_{\mu\nu} X^{\mu\nu} \quad (18)$$

$$= -\frac{\alpha_x}{3\pi} \frac{\lambda^2 v}{m_1 m_2} \left(\frac{h}{\sqrt{2}} \right) X_{\mu\nu} X^{\mu\nu} , \quad (19)$$

where $\Delta b_i = -4/3$, and corresponds to the gauge invariant effective operator

$$\mathcal{L}_{eff} \supset -\frac{\alpha_x}{6\pi} \frac{\lambda^2}{m_1 m_2} H^\dagger H X_{\mu\nu} X^{\mu\nu} . \quad (20)$$

We find the same result from the appropriate limit of the full loop calculation.¹ The expression of Eq. (20) shows that in the heavy fermion limit, the $h \rightarrow XX$ decay amplitude

¹ Our result is smaller by a factor of two than the related calculation of Ref. [36].

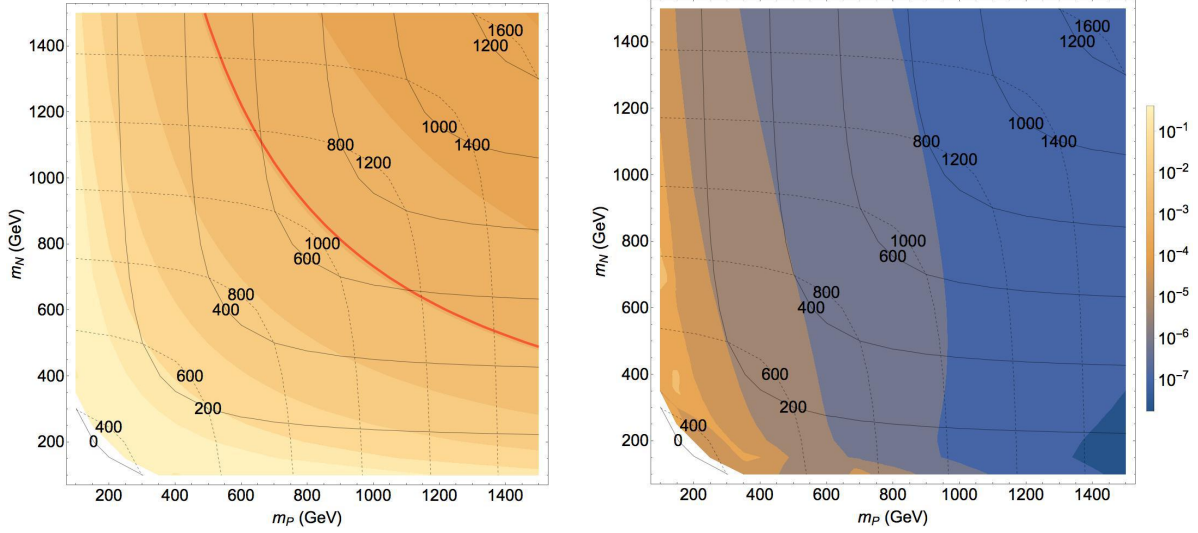


Figure 1: Branching ratios for $h \rightarrow XX$ (left) and $h \rightarrow XZ$ (right) decays due to mediator fermion loops in the m_P - m_N plane for $\lambda = 1$, $\alpha_x = 10\alpha$, and $m_x = 15$ GeV. The solid (dashed) black contours indicate m_1 (m_2) masses, while the solid red line shows the sensitivity of the most sensitive current LHC searches [46].

depends quadratically on the lepton portal Yukawa coupling λ and the dark gauge coupling g_x , and decouples if either of the neutral modes becomes very heavy. Both features arise from the non-diagonal Higgs coupling to the P and N fields. A similar low-energy calculation can be performed for the $h \rightarrow XZ$ mode, but the result is less illuminating and does not correspond to a single gauge-invariant operator. However, the result scales approximately quadratically in λ and linearly in g_x .

In Fig. 1 we show the range of Higgs branching fractions for $h \rightarrow XX$ (left) and $h \rightarrow XZ$ (right) in the m_P - m_N plane due to fermion loops for $\lambda = 1$, $\alpha_x = 10\alpha$, and $m_x = 15$ GeV. The solid (dashed) lines in the figure indicate contours of constant ψ_1 (ψ_2) masses. For the $h \rightarrow XX$ channel, the branching fractions are symmetric in m_P and m_N since both states couple equally to the dark vector. The decay fractions for $h \rightarrow XZ$ tend to be somewhat lower than for $h \rightarrow XX$, due to weaker effective couplings in the amplitudes for large α_x . In particular, the coupling of either fermion to the Z is at most $\bar{g}/2 < \sqrt{10\alpha_x}$ and is maximal for a doublet-like fermion, while the Higgs coupling relies on mixing between the P^0 and N gauge eigenstates.

These exotic Higgs decay channels to one or more dark vectors also arise from the standard vector and Higgs portal couplings [47, 48]. With only a vector portal, the main new decay is $h \rightarrow XZ$ through the SM $h \rightarrow ZZ$ vertex with one of the Z legs mixing into the dark vector X [49, 50]. The corresponding decay width is suppressed by both ϵ^2 and $(m_x/m_Z)^2$, and tends to have a very small branching fraction once other direct constraints on ϵ are taken into account [50]. The Higgs portal interaction can lead to $h \rightarrow XX$ decays with a significant rate [47, 48, 50]. We have not included the effects of these couplings in the results above. For minimal natural values of these parameters in our theory, we find that

their contributions to the Higgs decay amplitudes are much smaller than those from direct fermion loops over the range of masses shown in the figure.

3.2 Experimental Signals

Prospects for observing Higgs boson decays to one or more light dark vector bosons were studied in Refs. [33, 47, 48, 49, 50, 51, 52, 53, 54, 55]. If the X vector boson is the lightest state in the hidden sector, it decays exclusively to SM final states through its vector portal mixing with hypercharge. These decays can have a significant branching fraction to charged leptons [50], typically larger than that of the Z boson, and are prompt for natural values of the kinetic mixing ϵ .

The most recent experimental analysis of rare Higgs decays to dark vectors is the ATLAS study of Ref. [46], based on about 20.5 fb^{-1} of data at $\sqrt{s} = 8\text{ TeV}$. This search uses four-lepton final states with two opposite-sign same-flavor (OSSF) pairs, and covers the dark vector mass range $15\text{ GeV} \leq m_x \leq m_h/2$. For the $h \rightarrow XZ^{(*)}$ channel, the combined invariant mass is required to reconstruct the Higgs mass to within about 10 GeV, and a bump search is performed on the OSSF lepton pair with the lowest invariant mass. Their result can be translated into a limit on the branching ratio $\text{BR}(h \rightarrow XZ) \lesssim 0.5\text{--}5 \times 10^{-3}$ over the dark vector mass range covered by the search. In the $h \rightarrow XX$ channel, events with two OSSF pairs are also selected and grouped such that the resulting pair of two-body invariant masses are as close as possible. The exclusion derived corresponds to $\text{BR}(h \rightarrow XX) \lesssim 3 \times 10^{-4}$ over the vector mass range studied.

Comparing these LHC exclusions to the branching fractions found above due to the mediator fermions of the vectorized lepton portal, Fig. 1, we find that current data puts a significant limit on the new fermion masses for $\lambda = 1$ and $\alpha_x = 10\alpha$. Dedicated analyses with the full current and expected LHC data sets will have sensitivity to even larger fermion masses in both the $h \rightarrow XX$ and $h \rightarrow XZ$ channels. Let us also point out that the search of Ref. [46] concentrated on the dark vector mass range of $15\text{ GeV} \leq m_x \leq m_h/2$. This range is only weakly constrained by direct searches for dark vectors, with the strongest current bounds coming from precision electroweak tests that limit $\epsilon \lesssim 0.02$ [56]. The collider sensitivity to smaller dark vector masses is limited by backgrounds from heavy flavor resonances appearing at masses below about 11 GeV, and from the tendency of the leptons from a lighter vector boson to be collimated [57, 58]. Note, however, that existing direct limits on light dark vectors are much stronger for $m_x \lesssim 11\text{ GeV}$ and constrain $\epsilon \lesssim 10^{-3}$ [5], of the same size as the natural range for this coupling in our minimal theory.

Our analysis shows that exotic Higgs decays to dark vectors from loops of heavy mediator fermions are potentially observable in future Higgs searches at the LHC and beyond. In the sections to follow, we investigate other constraints on the theory from precision electroweak tests, direct collider searches, Higgs stability, and dark matter considerations. In doing so, we set $\lambda = 1$, $\alpha_x = 10\alpha$, and $m_x = 15\text{ GeV}$ as fiducial parameters against which to compare. For these parameters, we find that searches for exotic Higgs decay can provide comparable or greater sensitivity to the theory than other experimental probes.

4 Precision Electroweak and Collider Constraints

The vectorized lepton portal can induce significant decay fractions for $h \rightarrow XX$ and $h \rightarrow XZ$ provided λ and α_x are relatively large and the vector-like fermions ψ_1 and ψ_2 are not too heavy. In this section we investigate the bounds imposed on the theory from precision electroweak measurements, direct collider searches, and Higgs stability.

4.1 Electroweak Constraints

The new ψ_1 , ψ_2 , and P^- fermions couple directly to the electroweak vector bosons, and therefore induce oblique corrections to precision electroweak observables [59, 60]. In addition, the gauge kinetic mixing of $U(1)_x$ with hypercharge leads to mixing between the physical X , Z , and γ vector bosons, further modifying these observables [50, 56, 61, 62, 63]. However, for natural ranges of the kinetic mixing parameter $\epsilon \lesssim 10^{-2}$ with $m_x \lesssim 30$ GeV, the effects of vector boson mixing are much smaller than current limits [50, 56], and thus we focus exclusively on the effects of the heavy fermions.

Oblique corrections due to the new fermions are captured effectively by the Peskin-Takeuchi S , T , and U parameters. These have been computed for vector-like fermions with the same SM quantum numbers as those considered here in Refs. [20, 64]. Full expressions for the corrections to S , T , and U are collected in Appendix B.

To derive an exclusion on the theory from current electroweak data, we use the central values, uncertainties, and correlations among the S , T , and U parameters obtained in the fit of Ref. [65] with $m_t = 173$ GeV and $m_h = 125$ GeV. The corresponding 95% c.l. excluded region in the m_P - m_N plane for $\lambda = 1$ lies to the left of the solid black line in Fig. 2. We find that the corrections to S and U from the new fermions are typically very small, and the primary effect of the fermions is to shift the T parameter, related to the mass splitting of the components of the electroweak doublet P from mixing with N . Contours of ΔT are also shown in Fig. 2, and the excluded region is approximated well by the condition $\Delta T \lesssim 0.14$.

4.2 Collider Bounds

Collider searches for the charginos and neutralinos of supersymmetry can be applied to the vector-like fermions we are considering. In particular, our system consists of an electroweak doublet and singlet, and is similar in its collider phenomenology to a Higgsino-Bino system [41]. The lightest new fermion in the theory is ψ_1 , which is stable and contributes to missing energy in analogy to the lightest χ_1^0 neutralino. We estimate here the limits on the ψ_1 , ψ_2 , and P^- massive fermions by reinterpreting searches for electroweak superpartners at LEP II and the LHC.

For $m_P \ll m_N$, the lighter ψ_1 and P^- states both come mainly from the electroweak doublet and tend to be fairly close in mass, similar to a set of light Higgsinos ($\mu \ll M_1, M_2$). In contrast to light Higgsinos, however, the neutral state is a single Dirac fermion ψ_1 instead

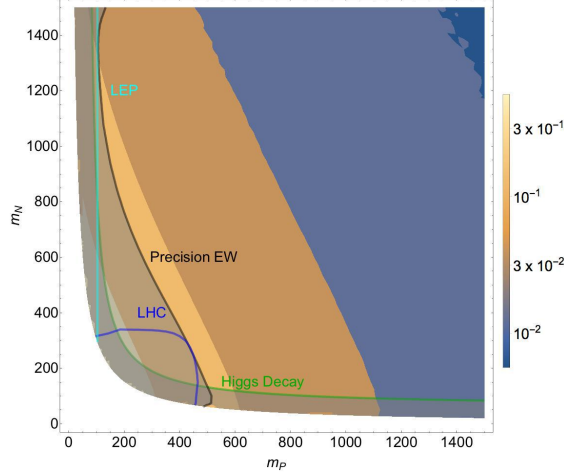


Figure 2: Precision electroweak and collider constraints on the minimal vectorized lepton portal for $\lambda = 1$. The dark grey line shows the combined exclusion from precision electroweak tests, the cyan (LEP) and blue (LHC) indicate bounds from direct collider searches, and the green line shows the limit from the non-observation of invisible Higgs decays. The coloured contours indicate the shifts in the oblique ΔT parameter due to the heavy fermions.

of a pair of Majorana χ_1 and χ_2 modes. The charged P^- state is similar to the lightest chargino χ_1^+ in its production, with decays through $P^- \rightarrow W^{(*)}\psi_1$. The heaviest state ψ_2 is mostly singlet, and will therefore have suppressed production through electroweak vector bosons. With $m_P \ll m_N$, it decays in a roughly 2 : 1 : 1 proportion via $\psi_2 \rightarrow W^+P^-$, $\psi_2 \rightarrow Z\psi_1$, and $\psi_2 \rightarrow h\psi_1$ [66].

In the opposite limit, $m_P \gg m_N$, the lightest state ψ_1 is mostly singlet while the heavier P^- and ψ_2 particles are Higgsino-like. They decay via $P^- \rightarrow W^-\psi_1$, along with $\psi_2 \rightarrow Z\psi_1$ and $\psi_2 \rightarrow h\psi_1$ in a roughly 1 : 1 ratio [66]. This system is similar to the electroweakino sector of a supersymmetric theory with $M_1 \ll \mu \ll M_2, m_{\text{fermion}}$.

Searches for superpartners at LEP II are summarized in Ref. [67]. The most relevant channels for our scenario are the chargino modes $e^+e^- \rightarrow \chi_1^+\chi_1^-$ with $\chi_1^+ \rightarrow \chi_1^0 W^{(*)}$ [68]. These can be applied directly to P^+P^- production. For $\lambda = 1$ and $m_N \lesssim 2$ TeV, the chargino limits translate into

$$m_P > 103 \text{ GeV} . \quad (21)$$

This value of λ (and the condition $\sqrt{m_N m_P} > \lambda v$ mentioned in Sec. 2) also implies that $(m_1 + m_2)$ is always larger than the maximal LEP II center-of-mass energy, so no bounds are obtained from searches for $\chi_1^0\chi_2^0$ production in this case. Searches for neutralino LSPs with initial-state photon radiation can also be applied to $e^+e^- \rightarrow \psi_1\bar{\psi}_1\gamma$ [69], but we find production cross sections well below the limit from Ref. [70].

More recently, the LHC collaborations have extended the constraints on electroweak superpartners to masses beyond the reach of LEP II. The new fermions in our theory can be produced by electroweak Drell-Yan channels, through an off-shell Higgs boson [71, 72, 73],

and via an s -channel dark vector. Whenever the production cross section is large enough to be potentially observable, we find that it is dominated by standard Drell-Yan (for fiducial values of $\lambda = 1$ and $\epsilon = 10^{-3}$). Decays of the heavier fermions to the stable ψ_1 produce signals with jets, leptons, and missing energy in direct analogy to supersymmetric cascades. Radiation of dark vectors by these fermions can produce additional visible objects in the events [14, 15, 16]. We do not expect such radiation to have a significant qualitative effect on the searches considered here that rely mainly on leptons that reconstruct a Z boson, but they could open new search channels at the LHC.

The most constraining LHC search for our theory appears to be the CMS opposite-sign same-flavor (OSSF) dilepton analysis of Ref. [74]. This search was based on 35.9 fb^{-1} of data at a center-of-mass energy of $\sqrt{s} = 13 \text{ TeV}$. The channels in the analysis relevant for our theory were those designed for $\chi_2^0 \chi_1^\pm$ production followed by $\chi_2^0 \rightarrow \chi_1^0 Z$ and $\chi_1^\pm \rightarrow \chi_1^0 W^\pm$. These channels required exactly two isolated light-flavor OSSF leptons with $86 \text{ GeV} < m_{\ell\ell} < 96 \text{ GeV}$, at least two jets with $p_T > 35 \text{ GeV}$ and $m_{jj} < 110 \text{ GeV}$, and missing energy $\cancel{E}_T > 100 \text{ GeV}$. Vetoes on additional leptons and b -tagged jets were also applied. These channels will receive contributions from $\bar{\psi}_2 P^-$ and $\psi_2 \bar{\psi}_2$ production with one on-shell $\psi_2 \rightarrow Z\psi_1$ decay.

To estimate exclusion limits from this search, we use `MadGraph5_aMC@NLO` [75] with a model implemented in `FeynRules` [76] to compute the relevant LHC production cross sections at $\sqrt{s} = 13 \text{ TeV}$. We then compare to the cross section limits obtained in Ref. [74] for a Wino-like $\chi_2^0 \chi_1^\pm$ simplified model in which the two electroweakino states are degenerate and assumed to decay exclusively to a stable χ_1^0 state through the weak vector bosons. In making the comparison, we include $P^- \bar{\psi}_2$, $P^+ \psi_2$, and $\psi_2 \bar{\psi}_2$ production, and we rescale their cross sections by the branching fraction for $\psi_2 \rightarrow Z\psi_1$. The main simplification we make in deriving our exclusions is the assumption that the detection efficiencies are approximately the same in our theory as for the simplified electroweakino model. We also take the exclusion cross section to be $\sigma_{tot} < 0.01 \text{ pb}$. Both assumptions are somewhat aggressive, and thus we expect our result to represent an upper limit on the exclusion derived from a full recasting of the CMS search. Our result is shown in Fig. 2.

Other potentially relevant LHC searches are the trilepton analysis of Ref. [77] and the mass-degenerate dilepton analysis of Ref. [78]. Comparing their excluded cross sections to those of our theory, we do not find any limits beyond the dilepton analysis described above.

4.3 Higgs Stability

New fermions with large Yukawa couplings to the Higgs field can destabilize the Higgs potential. They do so by modifying the renormalization group (RG) evolution of the Higgs self coupling λ_H , and tend to drive it negative at a lower scale than in the SM [79, 80, 81, 82]. Without additional new physics near the scale at which this occurs, the tunnelling rate from the standard electroweak vacuum to the unstable region at large Higgs field values tends to be shorter than the age of the universe [83, 84]. At best, this instability can be taken to be an upper cutoff for the consistency of the theory.

To investigate these effects, we evolve the couplings of the theory to higher scales using the one-loop RG equations for the system. These are listed in Appendix C, and generalize the results of Refs. [85, 86, 87]. As inputs, we use the \overline{MS} values for the relevant SM parameters derived in Ref. [88] defined at scale $\mu_t = 173.34$ GeV:

$$\begin{aligned} g_1 &= \sqrt{5/3} (0.3585) , & g_2 &= 0.6476 , & g_3 &= 1.1667 , \\ y_t &= 0.9369 , & \lambda_H &= 0.12597 . \end{aligned} \quad (22)$$

These inputs are evolved up to the fiducial massive fermion scale $\mu_F = 500$ GeV as in the SM, and then from μ_F to higher scales in the full theory with heavy fermions and the dark vector boson.

As expected, we find that the new Yukawa coupling λ drives the Higgs quartic coupling λ_H negative more quickly than in the SM. The condition we apply for the metastability of the standard electroweak vacuum follows Ref. [82], which is based on Ref. [83],

$$\lambda_H(\Lambda_H) = -0.065 [1 - 0.02 \ln(\Lambda_H/\mu_t)] . \quad (23)$$

This relation defines Λ_H , the maximum scale at which new physics that stabilizes the Higgs potential must emerge. Numerically, Λ_H tends to be one or two orders of magnitude larger than the scale at which the Higgs quartic coupling λ_H runs negative [84].

For the inputs listed in Eq. (22) together with $\lambda = 1$ and $\alpha_x = 10\alpha$ at μ_t , we find a Higgs instability cutoff scale of $\Lambda_H \simeq 4.6 \times 10^4$ GeV, with the quartic coupling running negative at $\mu \simeq 1.0 \times 10^4$ GeV. There is also a Landau pole in the new gauge coupling at scale $\mu \simeq 10^{11}$ GeV for $\alpha_x(\mu_t) = 10\alpha$. Reducing $\alpha_x(\mu_t)$ quickly pushes up the scale at which the Landau pole occurs, but has only a mild (lowering) effect on Λ_H . The Higgs instability scale for $\lambda = 1$ is relatively low, but is still high enough to justify our treatment of the heavy fermions provided we interpret the theory as an effective one with a cutoff near 5 TeV. Even so, we note that $\lambda = 1$ is close to the upper limit of what is possible for the consistency of our previous analyses.²

5 Connections to Dark Matter

In the minimal realization of the vectorized lepton portal, the lightest exotic fermion ψ_1 is stable and contributes to the density of dark matter (DM). This state is also a Dirac fermion with direct couplings to the Z^0 and X vector bosons, implying that it can have a large spin-independent scattering cross section with nuclei. We investigate these features in this section and show that they impose strong constraints on the model assuming standard thermal production of ψ_1 in the early universe. These constraints can be evaded in scenarios with low effective reheating temperatures or by going beyond the minimal realization of the theory.

²There is a significant sensitivity of these results to the SM input parameter values for small $\lambda \ll 1$ reflecting a theoretical uncertainty on our one-loop treatment. However, for $\lambda \sim 1$, the new Yukawa coupling dominates and the dependence on the SM inputs becomes modest.

5.1 Relic Densities

The relic density of ψ_1 particles from thermal freeze-out is determined by its dominant annihilation cross sections to dark vectors, electroweak vectors, and Higgs final states. Annihilation to pairs of dark vector bosons in our scenario is identical to minimal models of secluded dark matter [8], with leading cross section

$$\langle\sigma v\rangle_{XX} \simeq \frac{\pi\alpha_x^2}{m_1^2} \sqrt{1 - \left(\frac{m_x}{m_1}\right)^2}. \quad (24)$$

The complete expression can be found in Ref. [89]. Since both the N and P states couple in the same way to the dark vector, this cross section is independent of their mixing, and depends only on the gauge coupling α_x and the mass m_1 .³

For direct annihilation to SM final states, the most important modes are typically $\psi_1\bar{\psi}_1 \rightarrow ZZ, WW, hh$. These cross sections depend sensitively on the mixing between the P^0 and N gauge eigenstates that combine to make up ψ_1 and ψ_2 . The s -wave amplitude for the WW channel is facilitated by a t -channel P^- exchange and scales proportionally to s_α^2 , while the analogous ZZ process involves t -channel ψ_1 or ψ_2 exchange and is proportional to s_α^4 or $s_\alpha^2 c_\alpha^2$ respectively. In the event of small mixing angles, p -wave processes involving an s -channel Higgs can be significant. These amplitudes scale as $\lambda s_\alpha c_\alpha$, and include WW, ZZ , or hh final states.

In Fig. 3 we show regions in the $m_P - m_N$ plane where the ψ_1 relic density exceeds the observed value. In this figure, we set $\lambda = 1$ (left) and $\lambda = 0.1$ (right), with $m_x = 11$ GeV and several values of $\alpha_x = 0.1\alpha, \alpha, 3\alpha$. Setting $\alpha_x = 10\alpha$, the annihilation to dark vectors becomes very efficient and the entire parameter region shown yields an acceptable relic density. Also shown are contours of the ψ_1 mass m_1 .

5.2 Direct Detection

Direct searches for DM scattering put strong bounds on spin-independent DM-nucleon effective cross sections, on the order of $\sigma_{SI} \lesssim 10^{-46} \text{ cm}^2$ for $m_{DM} \sim 100$ GeV. This is orders or magnitude larger than the effective per-nucleon cross section of a stable Dirac fermion with electroweak charge, $\sigma_{SI} \simeq 10^{-39} \text{ cm}^2$ [93]. As a result, current direct detection bounds are sensitive to Dirac fermion relics that make up only a tiny fraction of the full dark matter density [94].

The spin-independent nucleon cross section of the ψ_1 state receives contributions from Z , X , and Higgs exchange. The corresponding effective operators have the same non-relativistic limit and interfere with each other. Together, they imply an effective per-nucleon cross

³ A light dark vector coupled to heavier dark matter can also enhance the annihilation cross section (in all channels) by the Sommerfeld effect [90, 91, 92]. We find that this enhancement is very mild for $\alpha_x \leq 10\alpha$ and $m_x = 15$ GeV.

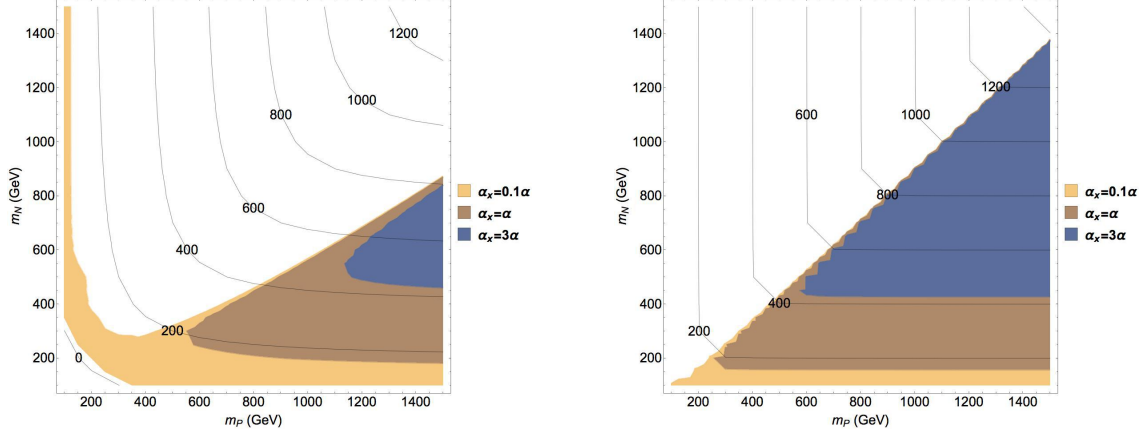


Figure 3: Regions in the m_P - m_N where the thermal ψ_1 relic density exceeds the observed value. The plot on the left has $\lambda = 1$, while the plot on the right corresponds to $\lambda = 0.1$. The different shadings show the exclusions for $\alpha_x = 0.1\alpha, \alpha, 3\alpha$. Also shown are contours of the ψ_1 mass m_1 .

section of [93]

$$\sigma_{SI} = \frac{\mu_n^2}{\pi} \left[\frac{f_p Z + f_n (A - Z)}{A} \right]^2, \quad (25)$$

where μ_n is the DM-nucleon reduced mass, A and Z describe the target nucleus, and

$$f_p = \frac{G_F}{\sqrt{2}} s_\alpha^2 (1 - 4s_W^2) - \frac{4\pi}{m_x^2} \epsilon q_x \sqrt{\alpha \alpha_x} + \tilde{d}_p \left[\frac{2}{9} + \sum_q f_{T,q}^p \right], \quad (26)$$

$$f_n = -\frac{G_F}{\sqrt{2}} s_\alpha^2 + 0 + \tilde{d}_n \left[\frac{2}{9} + \sum_q f_{T,q}^n \right]. \quad (27)$$

In both expressions above, the first term is due to Z exchange, the second to X exchange, and the third to Higgs exchange. The X exchange terms depend on the sign of the dark charge of ψ_1 and assume $m_x \gtrsim 100$ MeV. For the Higgs exchange terms, the quantity $\tilde{d}_{p,n}$ is given by

$$\tilde{d}_{p,n} = \frac{m_{p,n}}{v} \frac{\lambda s_\alpha c_\alpha}{m_h^2}, \quad (28)$$

where the sums run over $q = u, d, s$, and the coefficients $f_{T,q}^N$ can be found in Refs. [95, 96, 97].

Combining these expressions with the relic densities calculated previously, we find density-weighted per-nucleon cross sections, $(\Omega_1/\Omega_{DM})\sigma_{SI}$, that are typically much larger than the current constraints from PandaX [98] and LUX [99]. This applies even for $\alpha_x = 10\alpha$ when the ψ_1 relic density is significantly smaller than the total dark matter density. Dark photon exchange dominates for smaller m_x and natural one-loop values of the kinetic mixing ϵ . Even

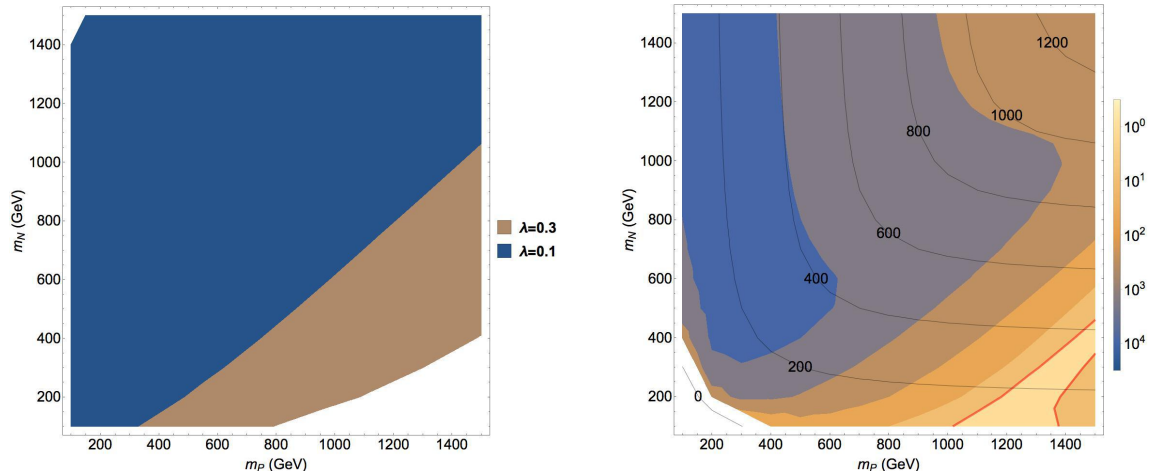


Figure 4: Two examples of how a thermal ψ_1 relic density with $\alpha_x = 10\alpha$ can be consistent with the current LUX bounds on spin-independent dark matter scattering [99]. The plot on the left illustrates the small λ scenario, in which $\epsilon \rightarrow 0$, the lighter ψ_1 state is very singlet-like with suppressed mixing with the doublet. The unshaded regions at the lower right for $\lambda = 0.1, 0.3$ where the ψ_1 state is mostly singlet are allowed by current bounds. The right panel illustrates the scenario where the contributions to nucleon scattering from the dark photon and the Z boson cancel against each other. This plot shows contours of $(\Omega_1/\Omega_{DM})\sigma_{SI}/\sigma_{LUX}$ for $\lambda = 1$, $\epsilon = 10^{-4}$, and $m_x = 10$ GeV. The allowed region between the solid red lines.

with this contribution suppressed by $\epsilon \rightarrow 0$, the scattering due to Z exchange still tends to be too large.

Two potential loopholes to these bounds exist. The first requires a very small $\epsilon \rightarrow 0$ to suppress dark photon exchange together with a lighter singlet-like ψ_1 state to reduce the Z and Higgs contributions to nucleon scattering. A large value of α_x is also needed to yield a small ψ_1 relic density. While these parameter values can give acceptably small density-weighted cross sections, they correspond to $s_\alpha \sim \lambda v/m_P \ll 1$ and imply a strong suppression of Higgs decays to dark photons. This is illustrated in the left panel of Fig. 4, where we show the parameter regions excluded by LUX [99] for $\lambda = 0.1, 0.3$, $\epsilon \rightarrow 0$, and $\alpha_x = 10\alpha$. The unshaded regions at the lower right are allowed.

The second loophole arises when there is a strong cancellation between the dark photon and Z boson contributions to the cross section. Suppression of the cross section from such a cancellation is limited by the mixture of isotopes present in natural xenon to about 2×10^{-4} relative to $f_p = f_n$. Moreover, the optimal suppression for xenon is different from that for other materials such as the germanium used in CDMS-II [100]. The allowed region of parameter space in this context for $\lambda = 1$, $\epsilon = 10^{-4}$, $m_x = 10$ GeV, and $\alpha_x = 10\alpha$ is illustrated in the right panel of Fig. 4, where we show contours of the density weighted spin-independent cross section relative to the bound from LUX [99], $(\Omega_1/\Omega_{DM})\sigma_{SI}/\sigma_{LUX}$. The region between the solid red lines is consistent with current limits.

5.3 Beyond the Minimal Scenario

Our analysis shows that the lightest ψ_1 fermion is very strongly constrained by dark matter direct detection, particularly when the Higgs branching fraction to dark vectors is significant. A similar conclusion was obtained in Ref. [17]. These constraints can be avoided if there is non-thermal cosmological evolution or additional structure in the theory.

The relic densities used in making the estimates above assumed thermal cosmological evolution during and after the freezeout of the stable ψ_1 state. Much smaller relic densities can arise from non-thermal evolution. For example, late reheating following a period of inflation or matter domination with a reheating temperature below the freeze-out temperature of ψ_1 can yield a relic density that is orders of magnitude below the thermal value [101]. Even so, the tiny remaining abundance of ψ_1 could still be observable in direct detection experiments due to its large spin-dependent scattering cross section [94].

Constraints on the ψ_1 abundance from direct detection can also be reduced if it obtains a small Majorana mass or is able to decay [17]. A Majorana mass for ψ_1 can arise from the dark Higgs coupling listed in Eq. (17). Such a mass term will split the four-component ψ_1 Dirac fermion into a pair of Majorana fermions, and thereby remove the dominant contribution to spin-independent elastic scattering from vector boson exchange [102]. The residual vector-mediated inelastic scattering is highly suppressed for mass splitting above about $\Delta m_1 > 200$ keV. We find that the remaining spin-independent scattering due to Higgs exchange can still be significant for $\lambda = 1$, but it can lie below current limits for the subleading ψ_1 relic densities that occur for $\alpha_x = 10\alpha$. Alternatively, the operator of Eq. (16) allows the ψ_1 state to decay to SM fermions through an electroweak vector boson, in which case the limits from dark matter searches are not relevant. While the coupling of Eq. (16) is constrained by searches for lepton flavor violation, it is not difficult to avoid these limits while ensuring that ψ_1 decays occur before the onset of primordial nucleosynthesis.

6 Comments on the Non-Abelian Case

The vectorized lepton portal can also connect the SM to non-Abelian dark gauge groups. This arises in some theories addressing electroweak naturalness [27, 28], typically with a dark gauge group of $G_x = SU(3)$, but the general structure can emerge more broadly [36, 103, 104, 105, 106]. These more general groups can produce important changes in experimental observables compared to $G_x = U(1)_x$. While many of these effects have been discussed in other contexts, we review them briefly here and point out a few particular features of our minimal construction. To be concrete, we focus here on $G_x = SU(N_x)$ with P and N transforming in a complex representation r , as discussed in Ref. [36, 104].

6.1 Higgs Decays to Dark Glueballs

Instead of dark photons, the new vector bosons will be analagous to gluons. If there is no symmetry breaking in the dark sector and no other matter fields, the *dark gluons* will confine to form *dark glueballs* at the scale Λ_x . Here and for the rest of this section, we assume $\Lambda_x \ll m_h$ so that the direct effects of the new fermions can be treated in perturbation theory, and we define α_x to be the running dark coupling at scale $\mu = m_h$. The dark confinement scale is approximately

$$\Lambda_x \simeq m_h \exp\left(-\frac{6\pi}{11N_x\alpha_x}\right). \quad (29)$$

This falls very quickly with decreasing α_x : for $N_x = 3$ we find $(\alpha_x, \Lambda_x) \simeq (15\alpha, 1 \text{ GeV})$, $(10\alpha, 75 \text{ MeV})$, $(6.2\alpha, 1 \text{ MeV})$, and $(\alpha, 10^{-27} \text{ MeV})$.

The lightest dark glueball has quantum numbers $J^{PC} = 0^{++}$ and mass (for $N_x = 3$) $m_0 \simeq 6.8\Lambda_x$ [107, 108], but several other metastable glueballs arise as well. The effective Higgs interaction induced by the N and P fermions can be obtained by generalizing the calculation of Sec. 3:

$$-\mathcal{L}_{eff} \supset \frac{\alpha_x T_2(r)}{6\pi} \frac{\lambda^2}{m_1 m_2} H^\dagger H X_{\mu\nu}^a X^{a\mu\nu}. \quad (30)$$

After confinement and electroweak symmetry breaking, this operator induces a Higgs portal coupling between the 0^{++} glueball and the SM Higgs boson, allowing it to decay with width [36]

$$\Gamma_{0^{++}} \simeq \left[\frac{T_2(r)}{6\pi} \frac{\lambda^2}{m_1 m_2} \right]^2 \left| \frac{\sqrt{2}v F_S}{m_0^2 - m_h^2 - i\Gamma_h m_h} \right|^2 \Gamma_h(m_0), \quad (31)$$

where $F_S \simeq (N_x/3)2.3m_0^3$ is a glueball matrix element determined on the lattice [108, 109], and $\Gamma_h(m_0)$ is the decay width the SM Higgs would have if its mass were equal to m_0 . Like the confinement scale, the glueball decay width varies extremely rapidly with the value of the running dark gauge coupling at m_h . Setting $\lambda = 1$ and $\sqrt{m_1 m_2} = 500 \text{ GeV}$, we find a lifetime of $\tau \simeq 1 \text{ s}$ for $\alpha_x(m_h) = 12\alpha$, and a decay length of $c\tau = 1 \text{ mm}$ for $\alpha_x(m_h) = 23\alpha$.⁴

Higgs decays to dark glueballs also proceed through the operator of Eq. (30) [110, 111]. For light glueball masses, $m_0 \ll m_h/2$, the inclusive glueball branching fraction follows that for decays to dark photons up to a simple rescaling:

$$\text{BR}(h \rightarrow \text{glueballs}) \simeq \text{BR}(h \rightarrow XX) \times \frac{T_2^2(r)(N_x^2 - 1)}{q_x^4}. \quad (32)$$

When m_0 approaches $m_h/2$, resonances in the final state can modify the branching fraction in important ways [110, 111]. Note as well that there is no $h \rightarrow (Z + \text{glueballs})$ decay

⁴Fermion loops also yield dimension-eight operators connecting the dark gluons to SM vector bosons, but these yield much smaller decay widths for the parameter ranges of interest [103, 104].

channel in the absence of gauge symmetry breaking in the dark sector. The glueball final states from Higgs decays tend to be long-lived and appear as simple missing energy unless $\alpha_x(m_h)$ is much larger than α . For moderate $\alpha_x(m_h)$, dedicated far detectors at the LHC could be sensitive to very late glueball decays [112]. Very large values of $\alpha_x(m_h)$ can give rise to displaced decays within ATLAS or CMS [110, 111], or produce emerging or semivisible jets [113, 114].

Other dark vector decay modes can arise when there is symmetry breaking in the dark sector above the confinement scale. For example, an adjoint dark Higgs field with a Yukawa coupling ξ to the N or P fermions gives rise to the operator

$$\mathcal{O} \sim \frac{\sqrt{\alpha_x \alpha} \xi T_2(r)}{4\pi} \frac{1}{m} \Phi^a X_{\mu\nu}^a B^{\mu\nu}, \quad (33)$$

where $m_\psi \sim m_1, m_2$. This produces a kinetic mixing interaction for $\Phi^a \rightarrow \langle \Phi^a \rangle$, and could allow more rapid decays of (some of) the dark vector bosons [9, 115, 116, 117].

6.2 Constraints

Bounds from precision electroweak tests and Higgs stability are mostly independent of the low-energy dynamics of the dark sector. The shifts in the oblique parameters discussed in Sec. 4.1 are enhanced by a factor of $d(r)$, the dimension of the G_x representation of N and P . For $G_x = SU(3)$ with $r = \mathbf{3}$ and $\lambda = 1$, this leads to an exclusion of $m_P \gtrsim 1000 - 400$ GeV for $m_N = 0 - 1500$ GeV.

The renormalization group equations relevant for a Higgs stability analysis with a general non-Abelian group G_x and fermion representation r are collected in Appendix C. For a given value of λ , the bound from Higgs stability rapidly becomes more stringent as the dimension of the fermion representation increases. With $G_x = SU(3)$, $r = \mathbf{3}$, $\lambda = 1$, and $\alpha_x = 10\alpha$, the Higgs stability cutoff approaches $\Lambda_H \simeq 3$ TeV, only slightly above the range of explicit fermion masses we are considering. This situation can be improved somewhat by lowering the new Yukawa coupling modestly; reducing to $\lambda = 0.8$ increases the stability cutoff scale to well over 10 TeV. The corresponding reduction in the Higgs branching fraction to dark vectors can be compensated by the color factors in Eq. (32) and an increased dark gauge coupling. Note as well that in theories with non-Abelian dark ($SU(3)$) gauge groups motivated by electroweak naturalness, new physics is typically expected at scales below about 10 TeV [27, 28, 110].

Direct collider searches for the massive fermions in the theory can be modified in more radical ways by an unbroken non-Abelian dark gauge group with $\Lambda_x \ll m_1, m_2$ [118, 119, 120]. Even so, we argue that our previous collider limits derived for the Abelian scenario can be applied here in many cases up to a rescaling by the fermion multiplicity $d(r)$. The first stages of fermion production and decay proceed much like in the Abelian case. Strong G_x dynamics does not have a significant effect on fermion production (away from threshold), with the fermions created in pairs primarily by Drell-Yan processes. Next, the heavier ψ_2 and P^- states decay down to the lightest ψ_1 mode. For non-degenerate fermion masses, this typically occurs before the non-perturbative G_x dynamics sets in.

The immediate remnants of fermion production and electroweak cascade decays are therefore a $\psi_1\bar{\psi}_1$ pair. In contrast to the Abelian theory where they would leave the detector as missing energy, the fermions are now *quirks* and remain bound by a string of G_x flux [118, 119, 120]. This string eventually pulls the fermions back together, causing them to oscillate until they annihilate [120]. Since the ψ_1 fermions do not carry colour or electromagnetic charge, they do not interact significantly with the material in collider detectors and they are not expected to be trapped. Their eventual annihilation products are dark glueballs, SM fermions, Higgs bosons, and W and Z vector bosons [120, 121, 122, 123, 124, 125]. For $\Lambda_x \gtrsim 1$ MeV, the dark glueball final states are the dominant decay products.

Our previous collider limits on the new fermions can be applied to the non-Abelian scenario as well when the dark glueballs are the dominant annihilation product and are long-lived. When these two conditions are met, the production modes and visible decay products are the nearly same as in the Abelian case up to an increased fermion multiplicity factor of $d(r)$. For $\Lambda_x \lesssim 1$ MeV, visible annihilation final states of the $\psi_1\bar{\psi}_1$ pair would provide an additional search channel [123, 125]. With larger $\Lambda_x \gtrsim 1$ GeV, displaced decays of the dark glueballs could be visible [125].

6.3 Dark Matter Considerations

Thermal freezeout of ψ_1 proceeds similarly to the Abelian case, and can be treated in perturbation theory for $\Lambda_x \ll m_1$. If the annihilation is dominated by $\psi\bar{\psi}_1 \rightarrow XX$ processes, the relic yield after freezeout is approximately

$$m_1 Y_1 = m_1 \left(\frac{n_1}{s} \right) \sim (10^{-11} \text{ GeV}) \left(\frac{m_1}{500 \text{ GeV}} \right)^2 \left(\frac{10\alpha}{\alpha_x} \right)^2. \quad (34)$$

As the early universe cools to below $T \lesssim \Lambda_x$ after freezeout, the dark flux connections among the relic ψ_1 and $\bar{\psi}_1$ states become important. These induce a second stage of $\psi_1\bar{\psi}_1$ annihilation to dark glueballs and SM final states [120, 126, 127].

For $\Lambda_x \gtrsim 100$ MeV, this secondary annihilation is expected to occur before the onset of primordial nucleosynthesis (BBN). However, smaller Λ_x produces a later stage of secondary annihilation, and the annihilation products can disrupt light element abundances [128, 129] or the cosmic microwave background radiation [130, 131]. We defer a full study of these effects to a future work, but we note that these considerations suggest that larger values of $\Lambda_x \gtrsim 100$ MeV are preferred if the new fermions and glueballs were ever thermalized in the early universe.⁵ Note that these constraints differ significantly from theories with quirks that carry QCD color, in which a second stage of QCD annihilation reduces the quirk relic densities to acceptable levels [120, 126, 127].

Cosmological constraints on relic fermions and glueballs can also be avoided if their pre-decay relic yield is significantly below the thermal estimate of Eq. (34). This can occur in scenarios with low reheating temperatures [101], or even from the heavy ψ_1 fermions themselves if they come to dominate the energy density of the universe before they decay [134].

⁵ Related considerations of relic glueball decays also tend to prefer larger Λ_x values [105, 106, 132, 133].

7 Conclusions

In this work we have studied the phenomenological consequences of the vectorized lepton portal, consisting of two or more new fermions that are charged under both the SM and a dark gauge force and that connect to the Higgs boson through a Yukawa coupling. The minimal realization consists of electroweak singlet and doublet fermions and an Abelian $U(1)_x$ dark gauge group. These fermions act as mediators between the visible and dark sectors, and they induce a gauge kinetic mixing of the $U(1)_x$ vector with hypercharge.

An important consequence of the mediator fermions is new exotic decay channels of the Higgs boson. In particular, fermion loops induce $h \rightarrow XX$ and $h \rightarrow XZ$ decays. The decay fractions of these modes are potentially observable at the LHC for larger values of the new Yukawa coupling λ and the dark gauge coupling α_x . We find that existing LHC searches for $h \rightarrow XX$ constrain the product of the new neutral fermion masses to be at least $\sqrt{m_1 m_2} \gtrsim 850$ GeV for $\lambda = 1$, $\alpha_x = 10\alpha$, and $m_x = 15$ GeV. This sensitivity to exotic Higgs decays can be significantly greater than direct limits on the new fermions from precision electroweak tests, collider searches, and Higgs stability considerations. Dark matter searches further constrain the new fermions, but the bounds depend on the evolution history of the cosmos. As a result, searches for exotic Higgs decays with future data from the LHC and beyond are a key discovery channel for scenarios of this type.

The minimal vectorized lepton portal studied here can also be extended in a number of ways. Expanding the new Yukawa coupling to a more general chiral form allows for CP violation in Higgs decays to dark vectors [17, 135]. If the dark sector has spontaneous symmetry breaking, the new fermions can potentially mix with SM leptons, leading to the violation of (charged) lepton flavor and introducing new interactions among neutrinos. The Abelian dark gauge group we have concentrated on can also be extended to non-Abelian groups with interesting consequences.

Acknowledgements

We thank Lindsay Forestell, David B. Kaplan, John Ng, Jessie Shelton, James Wells, and Richard Woloshyn for helpful discussions. This work is supported by the Natural Sciences and Engineering Research Council of Canada (NSERC), with DM supported in part by a Discovery Grant. TRIUMF receives federal funding via a contribution agreement with the National Research Council of Canada.

A Higgs Loop Functions

Higgs boson decays to $h \rightarrow XX$ and $h \rightarrow XZ$ are generated by loops of ψ_1 and ψ_2 fermions. All the relevant one-loop diagrams take the general form shown in Fig. 5, which connects the SM Higgs to a pair of vectors X and Y with internal fermion states a , b , and c . It

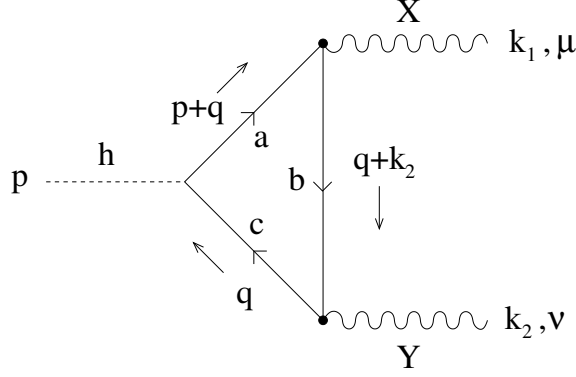


Figure 5: Loop diagram for $h \rightarrow XY$ decay due to the fermion loop $\{abc\}$.

corresponds to a contribution to the amplitude of

$$-i(\Delta\mathcal{M}) = g_{ach}g_{cbY}g_{baX} I^{\mu\nu} \varepsilon_\mu^*(k_1, \lambda_1) \varepsilon_\nu^*(k_2, \lambda_2) \quad (35)$$

with

$$I^{\mu\nu} = - \int \frac{d^d q}{(2\pi)^d} \frac{\text{tr}[(\not{q} + m_c)\gamma^\nu(\not{q} + \not{k}_1 + m_b)\gamma^\mu(\not{q} + \not{p} + m_a)]}{(q^2 - m_c^2 + i\varepsilon)[(q + k_1 - m_b)^2 + i\varepsilon][(q + p - m_a)^2 + i\varepsilon]} . \quad (36)$$

For each such diagram, there is a second independent diagram with the fermion arrows in Fig. 5 reversed of the form

$$II^{\mu\nu} = I^{\mu\nu}(a \leftrightarrow c, k_1 \leftrightarrow k_2, \mu \leftrightarrow \nu) . \quad (37)$$

Computing the diagram with dimensional regularization in $d = (4 - \epsilon)$, we find

$$I^{\mu\nu} = \frac{4i}{(4\pi)^2} \int_0^1 dx \int_0^{1-x} dy \left(\frac{1}{\Delta} (m_a m_b m_c \eta^{\mu\nu} + m_a A^{\mu\nu} + m_b B^{\mu\nu} + m_c C^{\mu\nu}) \right. \quad (38) \\ \left. - \eta^{\mu\nu} \left[(m_a + m_c - m_b) + (2m_b - m_a - m_c) \left(\frac{2}{\epsilon} + \dots \right) \right] \right) ,$$

where

$$A^{\mu\nu} = \left[-x^2 m_h^2 + (x + y - 2xy - y^2) m_Y^2 + (x - 2xy) (k_1 \cdot k_2) \right] \eta^{\mu\nu} \quad (39) \\ + (-x + 2x^2 + 2xy) k_1^\nu k_2^\mu$$

$$B^{\mu\nu} = \left[(-x + x^2) m_h^2 + (-y + 2xy + y^2) m_Y^2 + (-y + 2xy) (k_1 \cdot k_2) \right] \eta^{\mu\nu} \quad (40) \\ + y k_1^\nu k_2^\mu$$

$$C^{\mu\nu} = \left[(x - x^2) m_h^2 + (-1 + x + 2y - 2xy - y^2) m_Y^2 \right. \quad (41) \\ \left. + (-1 + x + y - 2xy) (k_1 \cdot k_2) \right] \eta^{\mu\nu} + (1 - 3x - y + 2x^2 + 2xy) k_1^\nu k_2^\mu$$

as well as

$$\begin{aligned}\Delta &= \Delta_{abc} = x m_a^2 + y m_b^2 + z m_c^2 \\ &\quad + (-x + x^2) m_h^2 + (-y + 2xy + y^2) m_Y^2 + 2xy (k_1 \cdot k_2) .\end{aligned}\tag{42}$$

The second loop $II^{\mu\nu}$ can be obtained from this result by exchanging $a \leftrightarrow c$ everywhere.

For $h \rightarrow XX$, the loops are $\{abc\} = \{111\}, \{222\}$. With $m_a = m_b = m_c$, we have $I^{\mu\nu}(aaa) = II^{\mu\nu}(aaa)$ and the would-be divergent parts in Eq. (38) cancel independently in each. The relevant coupling products are

$$g_{11h} g_{11X} g_{11X} = (-\sqrt{2}\lambda s_\alpha c_\alpha) g_x^2 \tag{43}$$

$$g_{22h} g_{22X} g_{22X} = (+\sqrt{2}\lambda s_\alpha c_\alpha) g_x^2 . \tag{44}$$

Note the relative sign.

In the case of $h \rightarrow XZ$, the loops are $\{abc\} = \{111\}, \{222\}, \{112\}, \{221\}$, and the relevant coupling products are

$$g_{11h} g_{11X} g_{11Z} = (-\sqrt{2}\lambda s_\alpha c_\alpha)(g_x q_x)(\bar{g} s_\alpha^2/2) \tag{45}$$

$$g_{22h} g_{22X} g_{22Z} = (+\sqrt{2}\lambda s_\alpha c_\alpha)(g_x q_x)(\bar{g} c_\alpha^2/2) \tag{46}$$

$$g_{21h} g_{11X} g_{12Z} = [\lambda(c_\alpha^2 - s_\alpha^2)/\sqrt{2}](g_x q_x)(-\bar{g} s_\alpha c_\alpha/2) \tag{47}$$

$$g_{12h} g_{22X} g_{21Z} = g_{21h} g_{11X} g_{12Z} , \tag{48}$$

where $\bar{g} = \sqrt{g^2 + g'^2}$. For $\{111\}$ and $\{222\}$, the would-be divergent terms in Eq. (38) cancel independently, while for $\{112\}$ and $\{221\}$ they cancel when the two contributions to the amplitude are summed.

B Electroweak Self-Energies

The relevant loop functions in $d = (4 - \epsilon)$ dimensions are

$$\begin{aligned}4\pi^2 L_{ab}(p^2) &= \left[\frac{1}{2}(m_a - m_b)^2 - \frac{1}{3}p^2 \right] \left[\frac{2}{\epsilon} - \gamma_E + \ln(4\pi) - \ln\left(\frac{p^2}{\mu^2}\right) \right] \\ &\quad + \left[(m_a m_b - m_a^2) \tilde{b}_0 + (m_a^2 - m_b^2 + 2p^2) \tilde{b}_1 - 2p^2 \tilde{b}_2 \right] ,\end{aligned}\tag{49}$$

where μ is the renormalization scale and

$$\tilde{b}_0(p, m_a, m_b) = \sum_{i=\pm} \left[\ln(1 - x_i) - x_i \ln\left(1 - \frac{1}{x_i}\right) - 1 \right] \tag{50}$$

$$2\tilde{b}_1(p, m_a, m_b) = \sum_{i=\pm} \left[\ln(1 - x_i) - x_i^2 \ln\left(1 - \frac{1}{x_i}\right) - x_i - \frac{1}{2} \right] \tag{51}$$

$$3\tilde{b}_2(p, m_a, m_b) = \sum_{i=\pm} \left[\ln(1 - x_i) - x_i^3 \ln\left(1 - \frac{1}{x_i}\right) - x_i^2 - \frac{x_i}{2} - \frac{1}{3} \right] \tag{52}$$

in which the index i labels

$$x_{\pm} = \frac{1}{2p^2} \left[(p^2 + m_a^2 - m_b^2) \pm \sqrt{(p^2 + m_a^2 - m_b^2)^2 - 4p^2(m_a^2 - i\varepsilon)} \right], \quad (53)$$

and the $i\varepsilon$ defines the proper branch of the logarithms when their arguments become negative or complex. These loop functions are closely related to (the finite parts) of the Passarino-Veltman functions [136]. For $p^2 \rightarrow 0$, the result simplifies to

$$\begin{aligned} 4\pi^2 L_{ab}(p^2) &= \frac{1}{2}(m_a - m_b)^2 \left[\frac{2}{\epsilon} - \gamma_E + \ln(4\pi) - \ln\left(\frac{m_a m_b}{\mu^2}\right) + \frac{1}{2} \right] \\ &\quad - \frac{1}{2} m_a m_b - \frac{1}{4(m_a^2 - m_b^2)} \ln\left(\frac{m_a^2}{m_b^2}\right) (m_a^4 - 2m_a^3 m_b - 2m_a m_b^3 + m_b^4). \end{aligned} \quad (54)$$

In terms of these loop functions, the shifts in the oblique parameters S , T , and U due to the vector-like fermions are [59, 60]

$$\begin{aligned} \Delta S &= \frac{4\pi}{m_Z^2} \left(-[L_{--}(m_Z^2) - L_{--}(0)] \right. \\ &\quad \left. + s_\alpha^4 [L_{11}(m_Z^2) - L_{11}(0)] + 2c_\alpha^2 s_\alpha^2 [12] + c_\alpha^4 [22] \right) \end{aligned} \quad (55)$$

$$\begin{aligned} \Delta S + \Delta U &= \frac{8\pi}{c_W^2 m_Z^2} \left(s_\alpha^2 [L_{1-}(m_W^2) - L_{1-}(0)] + c_\alpha^2 [L_{2-}(m_W^2) - L_{2-}(0)] \right. \\ &\quad \left. - c_W^2 [L_{--}(m_Z^2) - L_{--}(0)] \right) \end{aligned} \quad (56)$$

$$\Delta T = \frac{2\pi}{s_W^2 c_W^2 m_Z^2} \left[s_\alpha^2 L_{1-}(0) + c_\alpha^2 L_{2-}(0) - s_\alpha^2 c_\alpha^2 L_{12}(0) \right]. \quad (57)$$

These expressions are independent of $1/\epsilon$ and the renormalization scale μ .

C Renormalization Group Equations

We collect here the one-loop renormalization group (RG) equations relevant for the Higgs stability analysis of Sec. 4.3. In these equations, the only the SM Yukawa coupling we keep is that of the top quark, and we use the $SU(5)$ normalization for the hypercharge coupling, $g_1 = \sqrt{5/3} g'$. Our normalization for the Higgs self coupling is $V(H) \supset \lambda_H |H|^4$ so that $\lambda_H \simeq m_h^2/2v^2$ with $v \simeq 174$ GeV. To allow for generalization beyond the minimal Abelian vectorized lepton portal theory, we write the RG equations for general dark gauge group G_x under which P and N transform under the representation r_x with dimension $d(r_x)$.

With these assumptions, the RG equations for the system above the heavy fermion threshold can be adapted from the general results of Refs. [85, 86, 87] as in Refs. [79, 80, 81, 82].

We find

$$(4\pi)^2 \frac{d\lambda_H}{dt} = 24\lambda_H^2 + 4\lambda_H[3y_t^2 + 2d(r_x)\lambda^2] - 2[3y_t^4 + 2d(r_x)\lambda^4] - 3\lambda_H(3g_2^2 + \frac{3}{5}g_1^2) + \frac{3}{8} \left[2g_2^4 + (g_2^2 + \frac{3}{5}g_1^2)^2 \right] \quad (58)$$

$$(4\pi)^2 \frac{dy_t}{dt} = \frac{9}{2}y_t^3 + 2d(r_x)y_t\lambda^2 - y_t(8g_3^2 + \frac{9}{4}g_2^2 + \frac{17}{20}g_1^2) \quad (59)$$

$$(4\pi)^2 \frac{d\lambda}{dt} = \left[\frac{3 + 4d(r_x)}{2} \right] \lambda^3 + 3\lambda y_t^2 - \lambda \left[\frac{9}{4}g_2^2 + \frac{9}{20}g_1^2 + 6C_2(r_x)g_x^2 \right] , \quad (60)$$

together with

$$(4\pi)^2 \frac{dg_2}{dt} = \left[-\frac{19}{6} + \frac{2}{3}d(r_x) \right] g_2^3 \quad (61)$$

$$(4\pi)^2 \frac{dg_1}{dt} = \left[\frac{41}{10} + \frac{2}{5}d(r_x) \right] g_1^3 \quad (62)$$

$$(4\pi)^2 \frac{dg_x}{dt} = \left[-\frac{11}{3}C_2(G_x) + 4S_2(r_x) \right] g_x^3 , \quad (63)$$

where $t = \ln(\mu/\mu_0)$ defines the renormalization scale, and $S_2(r_x)$ and $C_2(r_x)$ refer to the trace and Casimir invariants of the representation r_x of N and P under G_x .

For $G_x = U(1)_x$ with N_f copies of the N and P fields of charge q_x , we have

$$C_2(r_x) = q_x^2 , \quad S_2(r_x) = q_x^2 N_f , \quad d(r_x) = N_f , \quad C_2(G_x) = 0 . \quad (64)$$

This case also allows for kinetic mixing between hypercharge and $U(1)_x$. The corresponding evolution equation for the mixing parameter $\tilde{\epsilon} = \epsilon/c_W$ above the heavy fermion mass threshold is [43, 44]

$$(4\pi)^2 \frac{d\tilde{\epsilon}}{dt} = 4N_f \tilde{\epsilon} (g_x q_x)^2 + \left(\frac{41}{10} + \frac{2}{5}N_f \right) \tilde{\epsilon} g_1^2 - \frac{8}{3} \sqrt{\frac{3}{5}} N_f g_1 (g_x q_x) . \quad (65)$$

Below the heavy fermion masses, the remaining evolution is homogeneous in $\tilde{\epsilon}$. There is also a small correction to the running of g_1 and g_x proportional to $\tilde{\epsilon}$ that we do not include.

References

- [1] P. Fayet, Phys. Rev. D **75**, 115017 (2007) doi:10.1103/PhysRevD.75.115017 [hep-ph/0702176 [HEP-PH]].
- [2] M. Pospelov, Phys. Rev. D **80**, 095002 (2009) doi:10.1103/PhysRevD.80.095002 [arXiv:0811.1030 [hep-ph]].

- [3] J. D. Bjorken, R. Essig, P. Schuster and N. Toro, Phys. Rev. D **80**, 075018 (2009) doi:10.1103/PhysRevD.80.075018 [arXiv:0906.0580 [hep-ph]].
- [4] R. Essig *et al.*, arXiv:1311.0029 [hep-ph].
- [5] J. Alexander *et al.*, arXiv:1608.08632 [hep-ph].
- [6] C. Boehm and P. Fayet, Nucl. Phys. B **683**, 219 (2004) doi:10.1016/j.nuclphysb.2004.01.015 [hep-ph/0305261].
- [7] N. Borodatchenkova, D. Choudhury and M. Drees, Phys. Rev. Lett. **96**, 141802 (2006) doi:10.1103/PhysRevLett.96.141802 [hep-ph/0510147].
- [8] M. Pospelov, A. Ritz and M. B. Voloshin, Phys. Lett. B **662**, 53 (2008) doi:10.1016/j.physletb.2008.02.052 [arXiv:0711.4866 [hep-ph]].
- [9] N. Arkani-Hamed, D. P. Finkbeiner, T. R. Slatyer and N. Weiner, Phys. Rev. D **79**, 015014 (2009) doi:10.1103/PhysRevD.79.015014 [arXiv:0810.0713 [hep-ph]].
- [10] L. B. Okun, Sov. Phys. JETP **56**, 502 (1982) [Zh. Eksp. Teor. Fiz. **83**, 892 (1982)].
- [11] B. Holdom, Phys. Lett. B **166**, 196 (1986). doi:10.1016/0370-2693(86)91377-8
- [12] R. M. Schabinger and J. D. Wells, Phys. Rev. D **72**, 093007 (2005) doi:10.1103/PhysRevD.72.093007 [hep-ph/0509209].
- [13] B. Patt and F. Wilczek, hep-ph/0605188.
- [14] M. J. Strassler and K. M. Zurek, Phys. Lett. B **651**, 374 (2007) doi:10.1016/j.physletb.2007.06.055 [hep-ph/0604261].
- [15] M. J. Strassler, hep-ph/0607160.
- [16] T. Han, Z. Si, K. M. Zurek and M. J. Strassler, JHEP **0807**, 008 (2008) doi:10.1088/1126-6708/2008/07/008 [arXiv:0712.2041 [hep-ph]].
- [17] H. Davoudiasl, H. S. Lee and W. J. Marciano, Phys. Rev. D **86**, 095009 (2012) doi:10.1103/PhysRevD.86.095009 [arXiv:1208.2973 [hep-ph]].
- [18] E. C. G. Stueckelberg, Helv. Phys. Acta **11**, 225 (1938). doi:10.5169/seals-110852
- [19] B. Kors and P. Nath, Phys. Lett. B **586**, 366 (2004) doi:10.1016/j.physletb.2004.02.051 [hep-ph/0402047].
- [20] S. A. R. Ellis, R. M. Godbole, S. Gopalakrishna and J. D. Wells, JHEP **1409**, 130 (2014) doi:10.1007/JHEP09(2014)130 [arXiv:1404.4398 [hep-ph]].
- [21] S. Bhattacharya, N. Sahoo and N. Sahu, Phys. Rev. D **93**, no. 11, 115040 (2016) doi:10.1103/PhysRevD.93.115040 [arXiv:1510.02760 [hep-ph]].

- [22] G. R. Dvali, G. F. Giudice and A. Pomarol, Nucl. Phys. B **478**, 31 (1996) doi:10.1016/0550-3213(96)00404-X [hep-ph/9603238].
- [23] N. Craig, S. Knapen, D. Shih and Y. Zhao, JHEP **1303**, 154 (2013) doi:10.1007/JHEP03(2013)154 [arXiv:1206.4086 [hep-ph]].
- [24] A. Azatov, J. Galloway and M. A. Luty, Phys. Rev. Lett. **108**, 041802 (2012) doi:10.1103/PhysRevLett.108.041802 [arXiv:1106.3346 [hep-ph]].
- [25] J. J. Heckman, P. Kumar, C. Vafa and B. Wecht, JHEP **1201**, 156 (2012) doi:10.1007/JHEP01(2012)156 [arXiv:1108.3849 [hep-ph]].
- [26] J. L. Evans, M. Ibe and T. T. Yanagida, Phys. Rev. D **86**, 015017 (2012) doi:10.1103/PhysRevD.86.015017 [arXiv:1204.6085 [hep-ph]].
- [27] G. Burdman, Z. Chacko, H. S. Goh and R. Harnik, JHEP **0702**, 009 (2007) doi:10.1088/1126-6708/2007/02/009 [hep-ph/0609152].
- [28] H. Cai, H. C. Cheng and J. Terning, JHEP **0905**, 045 (2009) doi:10.1088/1126-6708/2009/05/045 [arXiv:0812.0843 [hep-ph]].
- [29] P. W. Graham, D. E. Kaplan and S. Rajendran, Phys. Rev. Lett. **115**, no. 22, 221801 (2015) doi:10.1103/PhysRevLett.115.221801 [arXiv:1504.07551 [hep-ph]].
- [30] O. Antipin and M. Redi, JHEP **1512**, 031 (2015) doi:10.1007/JHEP12(2015)031 [arXiv:1508.01112 [hep-ph]].
- [31] B. Batell, G. F. Giudice and M. McCullough, JHEP **1512**, 162 (2015) doi:10.1007/JHEP12(2015)162 [arXiv:1509.00834 [hep-ph]].
- [32] K. Choi and S. H. Im, JHEP **1601**, 149 (2016) doi:10.1007/JHEP01(2016)149 [arXiv:1511.00132 [hep-ph]].
- [33] H. Davoudiasl, H. S. Lee, I. Lewis and W. J. Marciano, Phys. Rev. D **88**, no. 1, 015022 (2013) doi:10.1103/PhysRevD.88.015022 [arXiv:1304.4935 [hep-ph]].
- [34] A. DiFranzo, P. J. Fox and T. M. P. Tait, JHEP **1604**, 135 (2016) doi:10.1007/JHEP04(2016)135 [arXiv:1512.06853 [hep-ph]].
- [35] A. DiFranzo and G. Mohlabeng, JHEP **1701**, 080 (2017) doi:10.1007/JHEP01(2017)080 [arXiv:1610.07606 [hep-ph]].
- [36] J. E. Juknevich, JHEP **1008**, 121 (2010) doi:10.1007/JHEP08(2010)121 [arXiv:0911.5616 [hep-ph]].
- [37] H. Beauchesne, E. Bertuzzo and G. Grilli di Cortona, arXiv:1705.06325 [hep-ph].
- [38] R. Mahbubani and L. Senatore, Phys. Rev. D **73**, 043510 (2006) doi:10.1103/PhysRevD.73.043510 [hep-ph/0510064].

- [39] F. D’Eramo, Phys. Rev. D **76**, 083522 (2007) doi:10.1103/PhysRevD.76.083522 [arXiv:0705.4493 [hep-ph]].
- [40] R. Essig, Phys. Rev. D **78**, 015004 (2008) doi:10.1103/PhysRevD.78.015004 [arXiv:0710.1668 [hep-ph]].
- [41] T. Cohen, J. Kearney, A. Pierce and D. Tucker-Smith, Phys. Rev. D **85**, 075003 (2012) doi:10.1103/PhysRevD.85.075003 [arXiv:1109.2604 [hep-ph]].
- [42] H. Davoudiasl, H. S. Lee and W. J. Marciano, Phys. Rev. D **85**, 115019 (2012) doi:10.1103/PhysRevD.85.115019 [arXiv:1203.2947 [hep-ph]].
- [43] F. del Aguila, G. D. Coughlan and M. Quiros, Nucl. Phys. B **307**, 633 (1988) Erratum: [Nucl. Phys. B **312**, 751 (1989)]. doi:10.1016/0550-3213(88)90266-0
- [44] K. R. Dienes, C. F. Kolda and J. March-Russell, Nucl. Phys. B **492**, 104 (1997) doi:10.1016/S0550-3213(97)80028-4, 10.1016/S0550-3213(97)00173-9 [hep-ph/9610479].
- [45] M. A. Shifman, A. I. Vainshtein, M. B. Voloshin and V. I. Zakharov, Sov. J. Nucl. Phys. **30**, 711 (1979) [Yad. Fiz. **30**, 1368 (1979)].
- [46] G. Aad *et al.* [ATLAS Collaboration], Phys. Rev. D **92**, no. 9, 092001 (2015) doi:10.1103/PhysRevD.92.092001 [arXiv:1505.07645 [hep-ex]].
- [47] S. Gopalakrishna, S. Jung and J. D. Wells, Phys. Rev. D **78**, 055002 (2008) doi:10.1103/PhysRevD.78.055002 [arXiv:0801.3456 [hep-ph]].
- [48] D. Curtin *et al.*, Phys. Rev. D **90**, no. 7, 075004 (2014) doi:10.1103/PhysRevD.90.075004 [arXiv:1312.4992 [hep-ph]].
- [49] A. Falkowski and R. Vega-Morales, JHEP **1412**, 037 (2014) doi:10.1007/JHEP12(2014)037 [arXiv:1405.1095 [hep-ph]].
- [50] D. Curtin, R. Essig, S. Gori and J. Shelton, JHEP **1502**, 157 (2015) doi:10.1007/JHEP02(2015)157 [arXiv:1412.0018 [hep-ph]].
- [51] E. Gabrielli, M. Heikinheimo, B. Mele and M. Raidal, Phys. Rev. D **90**, no. 5, 055032 (2014) doi:10.1103/PhysRevD.90.055032 [arXiv:1405.5196 [hep-ph]].
- [52] S. Biswas, E. Gabrielli, M. Heikinheimo and B. Mele, JHEP **1506**, 102 (2015) doi:10.1007/JHEP06(2015)102 [arXiv:1503.05836 [hep-ph]].
- [53] S. Biswas, E. Gabrielli, M. Heikinheimo and B. Mele, Phys. Rev. D **93**, no. 9, 093011 (2016) doi:10.1103/PhysRevD.93.093011 [arXiv:1603.01377 [hep-ph]].
- [54] S. Biswas, E. Gabrielli, M. Heikinheimo and B. Mele, arXiv:1703.00402 [hep-ph].
- [55] M. D. Campos, D. Cogollo, M. Lindner, T. Melo, F. S. Queiroz and W. Rodejohann, arXiv:1705.05388 [hep-ph].

- [56] A. Hook, E. Izaguirre and J. G. Wacker, *Adv. High Energy Phys.* **2011**, 859762 (2011) doi:10.1155/2011/859762 [arXiv:1006.0973 [hep-ph]].
- [57] A. Falkowski, J. T. Ruderman, T. Volansky and J. Zupan, *JHEP* **1005**, 077 (2010) doi:10.1007/JHEP05(2010)077 [arXiv:1002.2952 [hep-ph]].
- [58] A. Falkowski, J. T. Ruderman, T. Volansky and J. Zupan, *Phys. Rev. Lett.* **105**, 241801 (2010) doi:10.1103/PhysRevLett.105.241801 [arXiv:1007.3496 [hep-ph]].
- [59] M. E. Peskin and T. Takeuchi, *Phys. Rev. Lett.* **65**, 964 (1990). doi:10.1103/PhysRevLett.65.964
- [60] M. E. Peskin and T. Takeuchi, *Phys. Rev. D* **46**, 381 (1992). doi:10.1103/PhysRevD.46.381
- [61] K. S. Babu, C. F. Kolda and J. March-Russell, *Phys. Rev. D* **57**, 6788 (1998) doi:10.1103/PhysRevD.57.6788 [hep-ph/9710441].
- [62] J. Kumar and J. D. Wells, *Phys. Rev. D* **74**, 115017 (2006) doi:10.1103/PhysRevD.74.115017 [hep-ph/0606183].
- [63] W. F. Chang, J. N. Ng and J. M. S. Wu, *Phys. Rev. D* **74**, 095005 (2006) Erratum: [*Phys. Rev. D* **79**, 039902 (2009)] doi:10.1103/PhysRevD.74.095005, 10.1103/PhysRevD.79.039902 [hep-ph/0608068].
- [64] C. Y. Chen, S. Dawson and E. Furlan, arXiv:1703.06134 [hep-ph].
- [65] M. Baak *et al.* [Gfitter Group], *Eur. Phys. J. C* **74**, 3046 (2014) doi:10.1140/epjc/s10052-014-3046-5 [arXiv:1407.3792 [hep-ph]].
- [66] N. Kumar and S. P. Martin, *Phys. Rev. D* **92**, no. 11, 115018 (2015) doi:10.1103/PhysRevD.92.115018 [arXiv:1510.03456 [hep-ph]].
- [67] LEPSUSYWG, ALEPH, DELPHI, L3 and OPAL experiments, <http://lepsusy.web.cern.ch/lepsusy/>
- [68] LEPSUSYWG, ALEPH, DELPHI, L3 and OPAL experiments, note LEPSUSYWG/01-03.1 <http://lepsusy.web.cern.ch/lepsusy/>
- [69] P. J. Fox, R. Harnik, J. Kopp and Y. Tsai, *Phys. Rev. D* **84**, 014028 (2011) doi:10.1103/PhysRevD.84.014028 [arXiv:1103.0240 [hep-ph]].
- [70] J. Abdallah *et al.* [DELPHI Collaboration], *Eur. Phys. J. C* **38**, 395 (2005) doi:10.1140/epjc/s2004-02051-8 [hep-ex/0406019].
- [71] M. R. Buckley, D. Feld and D. Goncalves, *Phys. Rev. D* **91**, 015017 (2015) doi:10.1103/PhysRevD.91.015017 [arXiv:1410.6497 [hep-ph]].

- [72] P. Harris, V. V. Khoze, M. Spannowsky and C. Williams, Phys. Rev. D **91**, 055009 (2015) doi:10.1103/PhysRevD.91.055009 [arXiv:1411.0535 [hep-ph]].
- [73] N. Craig, H. K. Lou, M. McCullough and A. Thalapillil, JHEP **1602**, 127 (2016) doi:10.1007/JHEP02(2016)127 [arXiv:1412.0258 [hep-ph]].
- [74] CMS Collaboration [CMS Collaboration], CMS-PAS-SUS-16-034.
- [75] J. Alwall *et al.*, JHEP **1407**, 079 (2014) doi:10.1007/JHEP07(2014)079 [arXiv:1405.0301 [hep-ph]].
- [76] A. Alloul, N. D. Christensen, C. Degrande, C. Duhr and B. Fuks, Comput. Phys. Commun. **185**, 2250 (2014) doi:10.1016/j.cpc.2014.04.012 [arXiv:1310.1921 [hep-ph]].
- [77] CMS Collaboration [CMS Collaboration], CMS-PAS-SUS-16-039.
- [78] CMS Collaboration [CMS Collaboration], CMS-PAS-SUS-16-048.
- [79] G. D. Kribs, T. Plehn, M. Spannowsky and T. M. P. Tait, Phys. Rev. D **76**, 075016 (2007) doi:10.1103/PhysRevD.76.075016 [arXiv:0706.3718 [hep-ph]].
- [80] M. Hashimoto, Phys. Rev. D **81**, 075023 (2010) doi:10.1103/PhysRevD.81.075023 [arXiv:1001.4335 [hep-ph]].
- [81] K. Ishiwata and M. B. Wise, Phys. Rev. D **84**, 055025 (2011) doi:10.1103/PhysRevD.84.055025 [arXiv:1107.1490 [hep-ph]].
- [82] N. Arkani-Hamed, K. Blum, R. T. D'Agnolo and J. Fan, JHEP **1301**, 149 (2013) doi:10.1007/JHEP01(2013)149 [arXiv:1207.4482 [hep-ph]].
- [83] G. Isidori, G. Ridolfi and A. Strumia, Nucl. Phys. B **609**, 387 (2001) doi:10.1016/S0550-3213(01)00302-9 [hep-ph/0104016].
- [84] D. Buttazzo, G. Degrassi, P. P. Giardino, G. F. Giudice, F. Sala, A. Salvio and A. Strumia, JHEP **1312**, 089 (2013) doi:10.1007/JHEP12(2013)089 [arXiv:1307.3536 [hep-ph]].
- [85] M. E. Machacek and M. T. Vaughn, Nucl. Phys. B **222**, 83 (1983). doi:10.1016/0550-3213(83)90610-7
- [86] M. E. Machacek and M. T. Vaughn, Nucl. Phys. B **236**, 221 (1984). doi:10.1016/0550-3213(84)90533-9
- [87] M. E. Machacek and M. T. Vaughn, Nucl. Phys. B **249**, 70 (1985). doi:10.1016/0550-3213(85)90040-9
- [88] S. P. Martin, Phys. Rev. D **93**, no. 9, 094017 (2016) doi:10.1103/PhysRevD.93.094017 [arXiv:1604.01134 [hep-ph]].
- [89] J. M. Cline, G. Dupuis, Z. Liu and W. Xue, JHEP **1408**, 131 (2014) doi:10.1007/JHEP08(2014)131 [arXiv:1405.7691 [hep-ph]].

- [90] H. Baer, K. m. Cheung and J. F. Gunion, Phys. Rev. D **59**, 075002 (1999) doi:10.1103/PhysRevD.59.075002 [hep-ph/9806361].
- [91] M. Lattanzi and J. I. Silk, Phys. Rev. D **79**, 083523 (2009) doi:10.1103/PhysRevD.79.083523 [arXiv:0812.0360 [astro-ph]].
- [92] A. Falkowski, J. Juknevich and J. Shelton, arXiv:0908.1790 [hep-ph].
- [93] G. Jungman, M. Kamionkowski and K. Griest, Phys. Rept. **267**, 195 (1996) doi:10.1016/0370-1573(95)00058-5 [hep-ph/9506380].
- [94] J. Halverson, N. Orlofsky and A. Pierce, Phys. Rev. D **90**, no. 1, 015002 (2014) doi:10.1103/PhysRevD.90.015002 [arXiv:1403.1592 [hep-ph]].
- [95] R. J. Hill and M. P. Solon, Phys. Rev. D **91**, 043505 (2015) doi:10.1103/PhysRevD.91.043505 [arXiv:1409.8290 [hep-ph]].
- [96] F. Bishara, J. Brod, B. Grinstein and J. Zupan, JCAP **1702**, no. 02, 009 (2017) doi:10.1088/1475-7516/2017/02/009 [arXiv:1611.00368 [hep-ph]].
- [97] P. Junnarkar and A. Walker-Loud, Phys. Rev. D **87**, 114510 (2013) doi:10.1103/PhysRevD.87.114510 [arXiv:1301.1114 [hep-lat]].
- [98] A. Tan *et al.* [PandaX-II Collaboration], Phys. Rev. Lett. **117**, no. 12, 121303 (2016) doi:10.1103/PhysRevLett.117.121303 [arXiv:1607.07400 [hep-ex]].
- [99] D. S. Akerib *et al.* [LUX Collaboration], Phys. Rev. Lett. **118**, no. 2, 021303 (2017) doi:10.1103/PhysRevLett.118.021303 [arXiv:1608.07648 [astro-ph.CO]].
- [100] Z. Ahmed *et al.* [CDMS-II Collaboration], Science **327**, 1619 (2010) doi:10.1126/science.1186112 [arXiv:0912.3592 [astro-ph.CO]].
- [101] G. B. Gelmini and P. Gondolo, Phys. Rev. D **74**, 023510 (2006) doi:10.1103/PhysRevD.74.023510 [hep-ph/0602230].
- [102] D. Tucker-Smith and N. Weiner, Phys. Rev. D **64**, 043502 (2001) doi:10.1103/PhysRevD.64.043502 [hep-ph/0101138].
- [103] A. E. Faraggi and M. Pospelov, Astropart. Phys. **16**, 451 (2002) doi:10.1016/S0927-6505(01)00121-9 [hep-ph/0008223].
- [104] J. E. Juknevich, D. Melnikov and M. J. Strassler, JHEP **0907**, 055 (2009) doi:10.1088/1126-6708/2009/07/055 [arXiv:0903.0883 [hep-ph]].
- [105] K. K. Boddy, J. L. Feng, M. Kaplinghat and T. M. P. Tait, Phys. Rev. D **89**, no. 11, 115017 (2014) doi:10.1103/PhysRevD.89.115017 [arXiv:1402.3629 [hep-ph]].
- [106] K. K. Boddy, J. L. Feng, M. Kaplinghat, Y. Shadmi and T. M. P. Tait, Phys. Rev. D **90**, no. 9, 095016 (2014) doi:10.1103/PhysRevD.90.095016 [arXiv:1408.6532 [hep-ph]].

- [107] C. J. Morningstar and M. J. Peardon, Phys. Rev. D **60**, 034509 (1999) doi:10.1103/PhysRevD.60.034509 [hep-lat/9901004].
- [108] Y. Chen *et al.*, Phys. Rev. D **73**, 014516 (2006) doi:10.1103/PhysRevD.73.014516 [hep-lat/0510074].
- [109] H. B. Meyer, JHEP **0901**, 071 (2009) doi:10.1088/1126-6708/2009/01/071 [arXiv:0808.3151 [hep-lat]].
- [110] N. Craig, A. Katz, M. Strassler and R. Sundrum, JHEP **1507**, 105 (2015) doi:10.1007/JHEP07(2015)105 [arXiv:1501.05310 [hep-ph]].
- [111] D. Curtin and C. B. Verhaaren, JHEP **1512**, 072 (2015) doi:10.1007/JHEP12(2015)072 [arXiv:1506.06141 [hep-ph]].
- [112] J. P. Chou, D. Curtin and H. J. Lubatti, Phys. Lett. B **767**, 29 (2017) doi:10.1016/j.physletb.2017.01.043 [arXiv:1606.06298 [hep-ph]].
- [113] P. Schwaller, D. Stolarski and A. Weiler, JHEP **1505**, 059 (2015) doi:10.1007/JHEP05(2015)059 [arXiv:1502.05409 [hep-ph]].
- [114] T. Cohen, M. Lisanti and H. K. Lou, Phys. Rev. Lett. **115**, no. 17, 171804 (2015) doi:10.1103/PhysRevLett.115.171804 [arXiv:1503.00009 [hep-ph]].
- [115] M. Baumgart, C. Cheung, J. T. Ruderman, L. T. Wang and I. Yavin, JHEP **0904**, 014 (2009) doi:10.1088/1126-6708/2009/04/014 [arXiv:0901.0283 [hep-ph]].
- [116] J. Choquette and J. M. Cline, Phys. Rev. D **92**, no. 11, 115011 (2015) doi:10.1103/PhysRevD.92.115011 [arXiv:1509.05764 [hep-ph]].
- [117] G. Barello, S. Chang and C. A. Newby, Phys. Rev. D **94**, no. 5, 055018 (2016) doi:10.1103/PhysRevD.94.055018 [arXiv:1511.02865 [hep-ph]].
- [118] L. B. Okun, JETP Lett. **31**, 144 (1980) [Pisma Zh. Eksp. Teor. Fiz. **31**, 156 (1979)].
- [119] L. B. Okun, Nucl. Phys. B **173**, 1 (1980). doi:10.1016/0550-3213(80)90439-3
- [120] J. Kang and M. A. Luty, JHEP **0911**, 065 (2009) doi:10.1088/1126-6708/2009/11/065 [arXiv:0805.4642 [hep-ph]].
- [121] S. P. Martin, Phys. Rev. D **83**, 035019 (2011) doi:10.1103/PhysRevD.83.035019 [arXiv:1012.2072 [hep-ph]].
- [122] R. Harnik, G. D. Kribs and A. Martin, Phys. Rev. D **84**, 035029 (2011) doi:10.1103/PhysRevD.84.035029 [arXiv:1106.2569 [hep-ph]].
- [123] K. Cheung, W. Y. Keung and T. C. Yuan, Nucl. Phys. B **811**, 274 (2009) doi:10.1016/j.nuclphysb.2008.11.029 [arXiv:0810.1524 [hep-ph]].

- [124] V. D. Barger, E. W. N. Glover, K. Hikasa, W. Y. Keung, M. G. Olsson, C. J. Suchyta, III and X. R. Tata, Phys. Rev. D **35**, 3366 (1987) Erratum: [Phys. Rev. D **38**, 1632 (1988)]. doi:10.1103/PhysRevD.35.3366, 10.1103/PhysRevD.38.1632.2
- [125] Z. Chacko, D. Curtin and C. B. Verhaaren, Phys. Rev. D **94**, no. 1, 011504 (2016) doi:10.1103/PhysRevD.94.011504 [arXiv:1512.05782 [hep-ph]].
- [126] C. Jacoby and S. Nussinov, arXiv:0712.2681 [hep-ph].
- [127] S. Nussinov and C. Jacoby, arXiv:0907.4932 [hep-ph].
- [128] M. Kawasaki, K. Kohri and T. Moroi, Phys. Rev. D **71**, 083502 (2005) doi:10.1103/PhysRevD.71.083502 [astro-ph/0408426].
- [129] K. Jedamzik, Phys. Rev. D **74**, 103509 (2006) doi:10.1103/PhysRevD.74.103509 [hep-ph/0604251].
- [130] X. L. Chen and M. Kamionkowski, Phys. Rev. D **70**, 043502 (2004) doi:10.1103/PhysRevD.70.043502 [astro-ph/0310473].
- [131] A. Fradette, M. Pospelov, J. Pradler and A. Ritz, Phys. Rev. D **90**, no. 3, 035022 (2014) doi:10.1103/PhysRevD.90.035022 [arXiv:1407.0993 [hep-ph]].
- [132] I. Garcia Garcia, R. Lasenby and J. March-Russell, Phys. Rev. D **92**, no. 5, 055034 (2015) doi:10.1103/PhysRevD.92.055034 [arXiv:1505.07109 [hep-ph]].
- [133] L. Forestell, D. E. Morrissey and K. Sigurdson, Phys. Rev. D **95**, no. 1, 015032 (2017) doi:10.1103/PhysRevD.95.015032 [arXiv:1605.08048 [hep-ph]].
- [134] A. Soni, H. Xiao and Y. Zhang, arXiv:1704.02347 [hep-ph].
- [135] M. B. Voloshin, Phys. Rev. D **86**, 093016 (2012) doi:10.1103/PhysRevD.86.093016 [arXiv:1208.4303 [hep-ph]].
- [136] G. Passarino and M. J. G. Veltman, Nucl. Phys. B **160**, 151 (1979). doi:10.1016/0550-3213(79)90234-7